Polyhedron 158 (2019) 193–207

Contents lists available at ScienceDirect

Polyhedron

journal homepage: www.elsevier.com/locate/poly

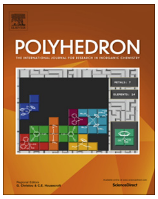

Thiophene site activation: Synthesis and structures of Fischer carbene complexes with 3,3′- and 2,3′-bithienyl substituents

Zandria Lamprecht [a], Mmushi M. Moeng [a], David C. Liles [a], Simon Lotz [a], Daniela I. Bezuidenhout [a,b,*]

[a] Chemistry Department, University of Pretoria, Private Bag X20, Hatfield 0028, Pretoria, South Africa
[b] Molecular Sciences Institute, School of Chemistry, University of the Witwatersrand, Johannesburg 2050, South Africa

ARTICLE INFO

Article history:
Received 24 September 2018
Accepted 21 October 2018
Available online 1 November 2018

Keywords:
Fischer carbene complexes
3,3′-Bithiophene
2,3′-Bithiophene
Group 6 transition metals
α-Activated thiophene sites

ABSTRACT

Deprotonation of the reactive α-thiophene ring positions of 3,3′-bithiophene and 2,3′-bithiophene afforded, after metalation with group 6 transition metal carbonyls and alkylation, a diverse range of mono- and biscarbene complexes. The bithienyl isomers differ in the number of active α-positions but representative examples of Fischer monocarbene complexes of all possible isomers were obtained. For 3,3′-bithienyl, the carbene fragment is in the electronically favoured C2-positions on the "inside" of the bithienyl and is structurally and electronically significantly different from the carbene substituent in the "outside" C5-positions. In the unsymmetrically substituted 2,3′-bithienyl scaffold, in addition to $[M(CO)_5\{C(OEt)\text{-}2'\text{-}(2,3'\text{-}BT)\}]$ and $[M(CO)_5\{C(OEt)\text{-}5'\text{-}(2,3'\text{-}BT)\}]$, a carbene moiety in the C5-position of the T2-thienyl ring, $[M(CO)_5\{C(OEt)\text{-}5\text{-}(2,3'\text{-}BT)\}]$, was also formed. In the same reaction mixture of the mono(ethoxycarbene) complexes, biscarbene complexes were obtained. In contrast, the major biscarbene complexes display the carbene fragments in the sterically favoured outside C5,C5′-positions. The unexpected formation of the 2,2′-bithienyl biscarbene complex, $[\{M(CO)_5C(OEt)\}_2\text{-}5,5'\text{-}(2,2'\text{-}BT)]$ as well as the formation of the biscarbene complexes $[\{M(CO)_5C(OEt)\}_2\text{-}2,5\text{-}(3,3'\text{-}BT)]$ and $[\{M(CO)_5C(OEt)\}_2\text{-}2',5'\text{-}(2,3'\text{-}BT)]$ with both carbene moieties on the same thiophene ring, were observed. By a modified method of synthesis, a mixed metal biscarbene complex of chromium and tungsten in the C2,C5-positions on the same thiophene ring could be isolated for both 3,3′-bithienyl and thiophene $[\{M_{a/b}(CO)_5C(OEt)\}_2\text{-}2,5\text{-}(T/3,3'\text{-}BT)]$. The formation of a monocarbene complex of 2,3′-bithienyl, $[W(CO)_5C(OEt)\text{-}5\text{-}(2,3'\text{-}BT)\{C(O)(OEt)\}_2\text{-}2',5']$ betrays the presence of an unstable triscarbene intermediate $[\{W(CO)_5C(OEt)\}_3\text{-}5,2',5'\text{-}(2,3'\text{-}BT)]$. The molecular structures of most of the major isomers were confirmed by single crystal X-ray studies.

1. Introduction

Thiophene is an electron rich molecule that acts as a net donor and displays strong conducting properties [1,2]. When attached to an electron withdrawing substituent (acceptor) and linked by a π-conjugated system, thiophene has the ability to delocalise electrons via π-resonance effects. Fischer mono- and biscarbene complexes bridged by oligothiophene units have been studied for their charge transfer properties (Fig. 1) [2]. For longer α,α′-thiophene chains, studies show that electron delocalization is often restricted and does not necessarily occur through the entire chain. Complexes with terminal biscarbene fragments (acceptors) with ter- and sexithiophene linkers, show that stabilization of the two competing electron withdrawing carbene units occurs predominately from the adjacent thiophene rings, leaving the central spacer thienyl rings essentially unaffected [3].

The above results prompted a careful investigation into the electronic and steric properties of bithienyl linkers in Fischer carbene (FC) complexes.

Bithienyl exists in three electronically different constitutional isomers shown in Fig. 2. Optimised *p*-orbital overlap requires the thienyl units to be planar for the three isomers and was confirmed in the solid state by X-ray diffraction studies [4]. The planar structures of the bithienyl isomers imply that inter-ring overlap (p_π-$p_{\pi'}$) leads to a bonding molecular orbital that includes both rings. A linear conjugated pathway is possible for the entire molecule in 2,2′-bithienyl that will include all olefinic bonds of the thiophene rings (Fig. 2b). In the case of 3,3′-bithienyl and 2,3′-bithienyl, π-resonance effects of this magnitude are not possible because the former allows for communication only between the C2 and

---

[*] Corresponding author at: University of the Witwatersrand, Molecular Sciences Institute, School of Chemistry, Johannesburg 2050, South Africa.

E-mail address: daniela.bezuidenhout@wits.ac.za (D.I. Bezuidenhout).

https://doi.org/10.1016/j.poly.2018.10.060
0277-5387/

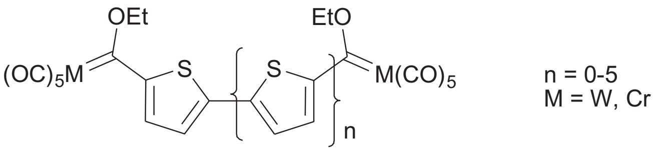

Fig. 1. Conjugated biscarbene complexes with α,α′-thienylene spacers.

C2′ positions, and the latter between C5 and C2′ (Fig. 2b). The reactivity of the three molecules was investigated by bromination, deuteration and deprotonation studies, and molecular orbital calculations used to predict the positions of substitution by determining the relative activation energies involved at the different sites [5]. The theoretical determined position of highest reactivity is found at the carbons of lowest activation energies, correlating with the experimental results. Reactions of the reference compound 2,2′-bithienyl (T2-T2′) occur at α-positions C5 (C5-C5′), for 3,3′-bithienyl (T3-T3′) at α-positions C2 (C2-C2′) and at the less reactive C5 (C5-C5′). For 2,3′-bithienyl (T2-T3′), the more reactive sites are at C2′ and C5′ on the T3′ ring and at C5 on the T2 ring (C5T2-C2′T3′, Fig. 2b). In this study, CX in CXTY-CX′TY′ (X, Y refer to site numbers) refers to a carbon atom (C), with a carbene substituent on a thiophene ring (T) in the X-position. Y refers to the site position where the two thiophene rings are connected. Atom numbering starts at the sulphur and proceeds in the direction passing the lower number (Y) for the connecting carbons of the two thiophene rings (T, T′). Discrimination of the thiophene rings is achieved by using a prime for the second thiophene ring in symmetrically substituted bithienyls. In the case of 2,3′-bithienyl, the primary thiophene ring is maintained as the T2 ring. The concept “*inside* versus *outside*” in this text refers to the number of ring sites available between the sulphur and thiophene-thiophene attachment positions with *inside* representing the smaller number of sites and *outside* the larger number of sites. The concept has structural implications (Fig. 2).

Table 1 summarises the number of active α-positions, the less reactive β-positions and the degree of conjugation in the thienyl rings of bithienyl for possible π-bond delocalisation. Table 1 also lists the number of Fischer carbene (FC) units reported (which can act as electron withdrawing moieties in activated positions) for the given bithienyls.

Unlike 2,2′-bithienyl, the 3,3′- and 2,3′-bithienyl stereoisomers are largely unexplored and have not yet been studied as substituents to carbene ligands in coordination chemistry. Fischer mono- and biscarbene complexes with 2,2′-bithienyl substituents are known for a range of transition metals [2,6,9–12]. Compared to 2,2′-bithienyl, the remaining two isomers, 3,3′- and 2,3′-bithienyl, have more α-reactive sites. Hence, more possible lithiation reactions could occur at different α-sites of similar reactivity and a greater variety of carbene complexes can be expected to form.

2. Experimental

2.1. Solvents and reagents

3-Bromothiophene, $CuCl_2 \cdot 6H_2O$, 2,3′-bithiophene, ammonia, dimethylammonium chloride, NaOH, *n*-BuLi (1.6 M solution in hexane) and group 6 metal carbonyls were purchased from Sigma Aldrich, Strem Chemicals and Afrox. Commercial bithienyls were tested for purity and composition by recording ^{1}H NMR spectra before use. All reagents were used as received, except $CuCl_2 \cdot 6H_2O$ was dried under vacuum while heat was applied. 3,3′-bithiophene [13] and triethyloxonium tetrafluoroborate [14] were prepared according to literature procedures and dimethylamine by an inhouse procedure [15]. All operations were carried out using standard Schlenk techniques under an inert atmosphere of nitrogen or argon. Silica gel 60 (particle size 0.063–0.20 mm) was used as resin for all column chromatography separations. Anhydrous THF (tetrahydrofuran), diethylether and hexane were distilled over sodium metal and benzophenone, and DCM (dichloromethane) over CaH_2.

2.2. Characterisation techniques

NMR spectra were recorded on Bruker ADVANCE 500, Ultrashield Plus 400 AVANCE 3 and Ultrashield 300 AVANCE 3 spectrometers, at 25 °C, using $CDCl_3$ as solvent. The ^{1}H NMR spectra were recorded at 500.139, 400.13 or 300.13 MHz, and the ^{13}C NMR spectra at 125.75, 100.613 or 75.468 MHz. The chemical shifts were referenced to deuterated chloroform ($CDCl_3$) signals at 7.26 ppm for δH and 77.00 ppm for δC. Coupling constants are reported in Hz. Numerical numbering of bithienylene atoms for NMR spectral assignments are indicated in Fig. 2a and in the Supplementary data, Fig. S4. Infrared spectroscopy was performed on a Bruker ALPHA FT-IR spectrophotometer with a NaCl cell, using hexane or DCM as solvent. Mass spectral analyses were performed on a Synapt G2 HDMS, by direct infusion at 10 μL/min, with

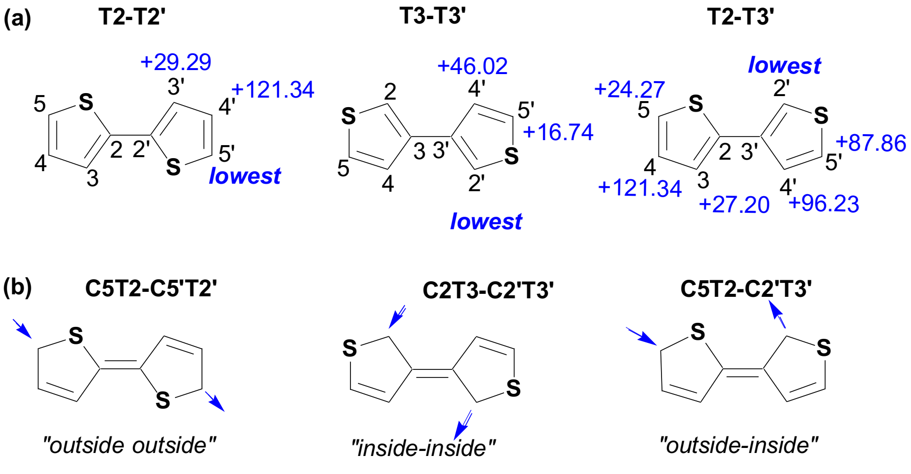

Fig. 2. (a) Molecular numbering scheme and site identification with the calculated relative activation energies (kJ/mol) [5]. (b) Examples of inter-ring delocalization of 2,2′-bithienyl, 3,3′-bithienyl and 2,3′-bithienyl indicating C site positions (arrows) when attached to substituents in α-positions.

Table 1
Active sites and stabilization of Fischer carbene (FC) fragments by conjugation at the different active sites.

	3,3′-Bithienyl **T3-T3′**	2,3′-Bithienyl **T2-T3′**	2,2′-Bithienyl [2,6] **T2-T2′**	Thiophene [7] **T**[a]
Structure	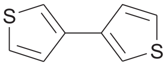	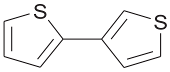	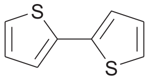	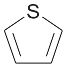
No. α-CH positions	4	3	2	2
No. β-CH positions	2	3	4	2
No. FC in α-C positions	This study	This study	2, 1	2, 1
Max no. of conjugated ring double bonds (Fig. 2).	2 (*inside-inside*)	3 (*inside-outside*)	4 (*outside-outside*)	2

[a] Protons in α-positions in thiophene are 500 times more acidic than those in β-positions [8].

negative electron spray as ionization technique. Samples were made up in 100% MeOH or acetonitrile to an approximate concentration of 10 μg/mL. The m/z values were measured in the range of 100–1500.

2.3. Crystal structure determination

Single crystal diffraction data were collected at 150 K on a Bruker D8 Venture diffractometer with a kappa geometry goniometer and a Photon 100 CMOS detector using a Mo Kα IμS.micro focus source. Data were reduced and scaled using SAINT [16]. Absorption corrections were performed using SADABS [16]. The structures were solved by a novel duel-space algorithm using SHELXTS [17] and were refined by full-matrix least-squares methods based on F^2 using SHELXL [18]. All non-hydrogen atoms were refined anisotropically. All hydrogen atoms were placed in idealised positions and refined using riding models.

2.4. Synthesis and characterization

2.4.1. General procedure for the synthesis of ethoxycarbene complexes

2.4.1.1. Method 1. A solution of bithiophene (1 equiv.) in THF was treated with *n*-BuLi (1.5 equiv.) at −78 °C. After stirring for 30 min, the metal carbonyl (1.5 equiv.) was added to the solution and stirred for a further 30 min in the cold and then allowed to reach room temperature over 40 min. The solvent was removed under reduced pressure and the residue dissolved in DCM and cooled to −20 °C. The reaction mixture was treated with $[Et_3O][BF_4]$ (1.5 equiv.) in DCM and subsequently allowed to reach room temperature. The reaction mixture was filtered through a small silica gel plug using DCM and the solvent was removed under reduced pressure. After absorbing the reaction mixture on silica, it was dry loaded onto a silica gel column. The products were separated by column chromatography using gradient elution with hexane and DCM.

2.4.1.1.1. Synthesis of 3,3′-bithiophene tungsten carbene complexes. 0.34 g (2.0 mmol) of 3,3′-bithiophene was dissolved in 15 mL THF, 1.90 mL (3.0 mmol) of *n*-BuLi and 1.06 g (3.0 mmol) $W(CO)_6$ were added. The reaction mixture was later dissolved in 10 mL DCM and 0.8 g (4.0 mmol) $[Et_3O][BF_4]$, dissolved in 10 mL DCM, was added. Column chromatography yielded six complexes. Compound **2a** first eluted, followed by **1a**, **12a**, **11a**, **10a** and **17a**.

1a: Yield: 0.37 g (0.68 mmol, 34%), red crystals. ν_{CO}(hexane)/cm^{-1} 2068 m ($A_1^{(1)}$), 1983vw (B_1), 1954sh ($A_1^{(2)}$), 1944vs (E). δ ^{1}H (300.13 MHz; $CDCl_3$; Me_4Si): 7.12 (1H, d, $^3J_{4,5}$ 5.0, H4), 7.71 (1H, d, $^3J_{5,4}$ 5.0, H5), 7.15 (1H, dd, $^4J_{2',5'}$ 3.0 and $^4J_{2',4'}$ 1.3, H2′), 6.94 (1H, dd, $^3J_{4',5'}$ 5.0 and $^4J_{4',2'}$ 1.3, H4′), 7.32 (1H, dd, $^3J_{5',4'}$ 5.0 and $^4J_{5',2'}$ 3.0, H5′), 4.71 (2H, q, ^3J 7.1, CH_2), 1.14 (3H, t, ^3J 7.1, CH_3). δ ^{13}C(75.468 MHz; $CDCl_3$; Me_4Si) 298.6 (C_{carb}), 202.6 (CO_{trans}), 197.4 (CO_{cis}), 156.8 (C2), 137.8 (C3), 131.6 (C4), 134.1 (C5), 122.4 (C2′), 133.5 (C3′), 128.5 (C4′), 125.2 (C5′), 79.0 (CH_2), 14.0 (CH_3). m/z($C_{16}H_{10}O_6S_2W$, 545.94 g/mol) 566.8801 (96%, $[M+Na-2H]^-$), 538.8760 (63%, $[M+Na-2H-CO]^-$), 482.9084 (100%, $[M+Na-2H-3CO]^-$).

2a: Yield: 0.19 g (0.35 mmol, 17%), red–purple crystals. ν_{CO}(hexane)/cm^{-1} 2067 m ($A_1^{(1)}$), 1981vw (B_1), 1954sh ($A_1^{(2)}$), 1944vs (E). δ ^{1}H(300.13 MHz; $CDCl_3$; Me_4Si): 7.83 (1H, d, $^4J_{2,4}$ 1.3, H2), 8.30 (1H, d, $^4J_{4,2}$ 1.4, H4), 7.46 (1H, dd, $^4J_{2',5'}$ 2.9 and $^4J_{2',4'}$ 1.3, H2′), 7.33 (1H, d, $^3J_{4',5'}$ 5.0, H4′), 7.41 (1H, dd, $^3J_{5',4'}$ 5.0 and $^4J_{5',2'}$ 2.9, H5′), 5.01 (2H, q, ^3J 7.1, CH_2), 1.68 (3H, t, ^3J 7.1, CH_3). δ ^{13}C(75.468 MHz; $CDCl_3$; Me_4Si) 290.6 (C_{carb}), 202.4 (CO_{trans}), 197.6 (CO_{cis}), 130.2 (C2), 139.2 (C3), 138.9 (C4), 158.5 (C5), 120.8 (C2′), 136.0 (C3′), 126.0 (C4′), 126.8 (C5′), 78.6 (CH_2), 15.0 (CH_3). m/z($C_{16}H_{10}O_6S_2W$, 545.94 g/mol) 566.8880 (75%, $[M+Na-2H]^-$), 538.8806 (45%, $[M+Na-2H-CO]^-$), 482.9099 (100%, [M+Na-2H-3CO].

10a: Yield: 0.52 g (0.56 mmol, 28%), purple-red crystals. ν_{CO}(hexane)/cm^{-1} 2064 m ($A_1^{(1)}$), 1982vw (B_1), 1955sh ($A_1^{(2)}$), 1946vs (E). δ ^{1}H(300.13 MHz; $CDCl_3$; Me_4Si) 7.87 (2H, d, $^4J_{2,4}$ 1.2, H2), 8.30 (2H, d, $^4J_{4,2}$ 1.2, H4), 5.03 (4H, q, ^3J 7.0, CH_2), 1.69 (6H, t, ^3J 7.0, CH_3). δ ^{13}C(75.468 MHz; $CDCl_3$; Me_4Si) 290.8 (C_{carb}), 202.3 (CO_{trans}), 197.5 (CO_{cis}), 130.4 (C2), 137.5 (C3), 138.8 (C4), 158.9 (C5), 78.7 (CH_2), 14.9 (CH_3). m/z($C_{24}H_{14}O_{12}S_2W_2$, 925.89 g/mol) 924.8770 (20%, $[M-H]^-$), 868.8815 (48%, $[M-H-2CO]^-$), 840.9309 (99%, $[M-H-3CO]^-$), 812.8959 (100%, [M−H−4CO]-).

11a: Yield: <3%, purple-red crystals. δ ^{1}H(400.13 MHz; $CDCl_3$; Me_4Si): 7.48 (1H, d, $^3J_{4,5\ 4.3}$, H4), 8.09 (1H, d, $^3J_{5,4\ 4.3}$, H5), 4.99 (2H, q, $^3J_{7.1}$, CH2), 1.68 (3H, t, $^3J_{7.1}$, CH3).

12a: Yield: <3%, purple-red crystals. δ ^{1}H(400.13 MHz; $CDCl_3$; Me_4Si) 7.10 (1H, d, $^3J_{4,5}$ 5.0, H4), 7.78 (1H, d, $^3J_{5,4}$ 5.0, H5), 7.56 (1H, d, $^4J_{2',4'}$ 1.2, H2′), 7.90 (1H, d, $^4J_{4',2'}$ 1.2, H4′), 4.72 (2H, q, ^3J 7.1, **C2**CH_2), 5.01 (2H, q, ^3J 6.9, **C5′**CH_2), 1.16 (3H, t, ^3J 7.1, **C2**CH_3), 1.67 (3H, t, ^3J 6.9, **C5′**CH_3).

17a: Yield: <3%, red crystals. δ ^{1}H(400.13 MHz; $CDCl_3$; Me_4Si) 8.02 (1H, s, H4), 7.61 (1H, dd, $^4J_{2',5'}$ 2.9 and $^4J_{2',4'}$ 1.3, H2′), 7.32 (1H, dd, $^3J_{4',5'}$ 5.0 and $^4J_{4',2'}$ 1.2, H4′), 7.37 (1H, dd, $^3J_{5',4'}$ 5.0 and $^4J_{5',2'}$ 3.0, H5′), 4.32 (2H, q, ^3J 7.0, C2-CH_2), 5.02 (2H, q, ^3J 7.0, C5-CH_2), 1.33 (3H, t, ^3J 7.2, C2-CH_3), 1.70 (3H, t, ^3J 7.1, C5-CH_3).

2.4.1.1.2. Synthesis of 2,3′-bithiophene tungsten carbene complexes. 0.33 g (2.0 mmol) of 2,3′-bithiophene was dissolved in 10 mL THF, 1.9 mL (3.0 mmol) of *n*-BuLi and 1.06 g (3.0 mmol) of W$(CO)_6$ were added. Dissolved in 20.00 mL DCM, the reaction was alkylated with 0.57 g (3.0 mmol) $[Et_3O][BF_4]$. Column chromatography yielded seven complexes. The monocarbene complexes: **3a, 4a**, and **5a** eluted first, followed by the biscarbene complexes: **14a**, **15a** and **16a**, along with a carbene with two ester groups **19a**.

3a: Yield: 0.22 g (0.4 mmol, 20%), orange-red crystals. ν_{CO}(hexane)/cm^{-1} 2067 m ($A_1^{(1)}$), 1981sh (B), 1955sh ($A_1^{(2)}$), 1944 s (E). δ ^{1}H (300 MHz; $CDCl_3$; Me_4Si) 6.97 (1H, dd, $^4J_{5,3}$ 1.1, $^3J_{4,3}$ 3.6, H3), 7.03 (1H, dd, $^3J_{\ 4,3}$ 3.6, $^3J_{4,5}$ 5.1, H4), 7.31 (1H, dd, $^4J_{5,3}$ 1.1, $^3J_{5,4}$ 5.1, H5), 7.16 (1H, d, $^3J_{4',5'}$ 5.1, H4′), 7.64 (1H, d, $^3J_{5',4'}$ 5.1, H5′), 4.76 (2H, q, ^3J 7.1, CH_2), 1.67 (3H, t, ^3J 7.1, CH_3). δ ^{13}C(100.613 MHz; $CDCl_3$; Me_4Si) 288.9 (C_{carb}), 202.5 (CO_{trans}), 197.2 (CO_{cis}). 149.5

(C2), 123.1 (C3), 125.1 (C4), 127.2 (C5), 155.2 (C2′), 143.7 (C3′), 131.4 (C4′), 134.6 (C5′), 78.1 (CH_2), 14.1 (CH_3).

4a: Yield: 0.12 g (0.2 mmol, 11%), red crystals. ν_{CO}(hexane)/cm^{-1} 2066 m ($A_1^{(1)}$), 1983sh (B), 1943 s (E). δ^{1}H(400 MHz; $CDCl_3$; Me_4Si) 7.26 (1H, $^3J_{5,3}$ 1.1, $^3J_{4,3}$ 3.7, dd, H3), 7.08 (1H, dd, $^3J_{4,3}$ 3.7, $^3J_{4,5}$ 5.1, H4), 7.28 (1H, dd, $^3J_{5,3}$ 1.1, $^3J_{5,4}$ 5.1, H5), 7.82 (1H, d, $^4J_{4',2'}$ 1.4, H2′), 8.25 (1H, d, $^4J_{2',4'}$ 1.4, H4′), 5.01 (2H, q, ^3J 7.1, CH_2), 1.68 (3H, t, ^3J 7.1, CH_3). δ^{13}C(100.613 MHz; $CDCl_3$; Me_4Si) 290.7 (C_{carb}), 202.4 (CO_{trans}), 197.5 (CO_{cis}), 137.6 (C2), 124.0 (C3), 125.0 (C4), 128.0 (C5), 129.6 (C2′), 138.2 (C3′), 137.2 (C4′), 158.6 (C5′), 78.7 (CH_2), 15.0 (CH_3). m/z($C_{16}H_{10}O_6S_2W$, 545.9428 g/mol), 545.9514 (27%, $[M]^-$), 517.9565 (28%, $[M-CO]^-$), 489.9644 (37%, $[M-2CO]^-$), 461.9698 (26%, $[M-3CO]^-$), 433.9734 (100%, $[M-4CO]^-$), 405.9771 (8%, $[M-5CO]^-$).

5a: Yield: 0.07 g (0.1 mmol, 6%), orange-brown crystals. ν_{CO}(hexane)/cm^{-1} 2065 m ($A_1^{(1)}$), 1955sh($A_1^{(2)}$), 1946 s (E). δ^{1}H (400 MHz; $CDCl_3$; Me_4Si) 7.33 (1H, d, $^3J_{3,4}$ 5.3, H3), 7.73 (1H, d, $^3J_{4,3}$ 5.3, H4), 7.39 (1H, dd, $^4J_{2',4'}$ 1.1, $^4J_{2',5'}$ 3.6, H2′), 7.35 (1H, dd, $^4J_{4',2'}$ 1.1, $^3J_{4',5'}$ 5.1, H4′), 7.57 (1H, dd, $^4J_{5',2'}$ 3.6, $^3J_{5',4'}$ 5.1, H5′), 5.07 (2H, q, ^3J 7.1, CH_2), 1.67 (3H, t, ^3J 7.1, CH_3). δ^{13}C (100.613 MHz; $CDCl_3$; Me_4Si) 288.4(C_{carb}), 202.4 (CO_{trans}), 147.1 (C5), 128.7 (C3), 141.5 (C4), 132.2 (C2′), 132.7 (C4′), 133.3 (C5′), 77.9 (CH_2), 15.1 (CH_3).

14a: Yield: 0.52 g (0.6 mmol, 28%), brown red crystals. ν_{CO}(hexane)/cm^{-1} 2064 m ($A_1^{(1)}$), 1984vw (B_1), 1955sh ($A_1^{(2)}$), 1944vs (E). δ^{1}H(400 MHz; $CDCl_3$; Me_4Si) 7.38 (1H, d, $^3J_{3,4}$ 4.3, H3), 8.15 (1H, d, $^3J_{4,3}$ 4.3, H4), 8.02 (1H, d, $^4J_{2',4'}$ 1.3, H2′), 8.26 (1H, d, $^4J_{4',2'}$ 1.3, H4′), 5.01 (2H, q, ^3J 7.0, CH_2), 5.03 (2H, q, ^3J 7.0, CH_2), 1.69 (3H, t, ^3J 7.0, CH_3), 1.68 (3H, t, ^3J 7.0, CH_3). δ^{13}C (100.613 MHz; $CDCl_3$; Me_4Si) 291.1(C-5′)(C_{carb}), 288.1(C-5)(C_{carb}), 202.5 and 202.2 (CO_{trans}), 197.6 and 197.3 (CO_{cis}), 147.3 (C2), 125.6 (C3), 143.4 (C3′), 156.3 (C5), 136.1 (C2′), 131.6 (C4), 137.0 (C4′), 159.5 (C5′), 78.9 and 78.4 (CH_2), 15.0 and 14.9 (CH_3). m/z($C_{24}H_{14}O_{12}S_2W_2$, 925.8946 g/mol), 925.9067 (51%, $[M]^-$), 897.9121 (100%, $[M-CO]^-$), 869.9167 (28%, $[M-2CO]^-$), 841.9157 (7%, $[M-3CO]^-$), 813.9256 (13%, $[M-4CO]^-$), 785.9268 (11%, $[M-5CO]^-$).

15a: Yield: 0.17 g (0.2 mmol, 9%), dark brown crystals. δ^{1}H (400 MHz; $CDCl_3$; Me_4Si) 7.03 (1H, dd, $^3J_{4,3}$ 3.8, H3) 7.05 (1H, dd, $^3J_{4,3}$ 3.6, $^3J_{4,5}$ 5.0, H4), 7.34 (1H, d, $^3J_{4,5}$ 5.0, H5), 7.98 (1H, s, H4′), 4.79 (2H, q, ^3J 6.5, CH_2), 1.38 (3H, t, ^3J 7.1, CH_3). δ^{13}C (100.613 MHz; $CDCl_3$; Me_4Si) 290.9 (C-5′)(C_{carb}), 305.8 (C-2′)(C_{carb}), 203.4 (CO_{trans}), 197.1 and 196.4 (CO_{cis}), 128.3 (C2), 126.8 (C3), 126.4 (C4), 127.4 (C5), 157.7 (C2′), 136.4 (C3′), 139.5 (C4′), 158.0 (C5′), 79.4 and 78.8 (CH_2), 14.9 and 14.2 (CH_3).

16a: Yield: 0.21 g (0.2 mmol, 11%), blue crystals. ν_{CO}(hexane)/cm^{-1} 2064 m ($A_1^{(1)}$), 1992vw (B_1), 1955 m ($A_1^{(2)}$), 1946vs (E). δ^{1}H (400 MHz; $CDCl_3$; Me_4Si) 8.09 (2H, d, $^3J_{3,4}$ 4.3, H3/H3′), 7.48 (2H, d, $^3J_{4,3}$ 4.3, H4/H4′), 5.00 (2H, q, ^3J 7.1, CH_2), 1.68 (3H, t, ^3J 7.1, CH_3). δ^{13}C(100.613 MHz; $CDCl_3$; Me_4Si) 288.5 (C_{carb}), 202.4 (CO_{trans}), 197.4 (CO_{cis}), 145.4 (C2), 127.0 (C3), 145.4 (C4), 157.8 (C5), 78.5 (CH_2), 15.0 (CH_3). m/z($C_{24}H_{14}O_{12}S_2W_2$), 925.8946 g/mol, 925.8946 (61%, $[M]^-$), 897.9146 (100%, $[M-CO]^-$), 869.9189 (39%, $[M-2CO]^-$), 841.9185 (15%, $[M-3CO]^-$), 813.9267 (12%, $[M-4CO]^-$), 785.9278 (14%, $[M-5CO]^-$).

19a: Yield: 0.08 g (0.1 mmol, 5%), reddish brown crystals. ν_{CO}(hexane)/cm^{-1} 2066 m ($A_1^{(1)}$), 1980vw (B_1), 1943 s (E). δ^{1}H (500 MHz; $CDCl_3$; Me_4Si) 7.61 (1H, d, $^3J_{3,4}$ 4.3, H3), 8.11 (1H, d, $^3J_{4,3}$ 4.3, H4), 7.88 (1H, s, H4′), 4.99 (2H, q, ^3J 7.1, CH_2), 1.66 (3H, t, ^3J 7.1, CH_3), 4.40 (2H, q, ^3J 7.1, CH_2), 1.40 (3H, t, ^3J 7.1, CH_3), 4.36 (2H, q, ^3J 7.1, CH_2), 1.36 (3H, t, ^3J 7.1, CH_3). δ^{13}C (100.613 MHz; $CDCl_3$; Me_4Si) 289.9 (C_{carb}), 202.6 (CO_{trans}), 197.5 (CO_{cis}), 161.1, ($CO_{(2')}$), 161.0 ($CO_{(5')}$), 145.3 (C2), 130.7 (C3), 141.7 (C4), 157.9 (C5), 133.4 (C2′), 137.1 (C3′), 135.3 (C4′), 138.2 (C5′), 78.5 (CH_2 (carbene)), 62.1 (CH_2 (ester)), 15.0 (CH_3), 14.2 (CH_3), 14.1 (CH_3). 689.9851 g/mol, 689.9951 (33%, $[M]^-$), 662.0050 (29%, $[M-CO]^-$), 635.0027 (100%, $[M+H\text{-}2CO]^-$), 578.0072 (32%, $[M-4CO]^-$).

In an effort to obtain pure triscarbene complex **18a** and to improve the yield, a 1:3 ratio of reagents (2,3′-bithiophene:n-BuLi/M(CO)$_6$) was also used, however without significant effect.

2.4.1.1.3. Synthesis of 3,3′-bithienyl chromium carbene complexes. 0.34 g (2.0 mmol) of 3,3′-bithiophene was dissolved in 15 mL THF, 1.90 mL (3.0 mmol) of n-BuLi and 0.67 g (3.0 mmol) $Cr(CO)_6$ were added. 0.8 g (4.0 mmol) $[Et_3O][BF_4]$, dissolved in 10 mL DCM, was added to the reaction mixture dissolved in DCM. Five complexes were isolated. Compound **2b** was first to elute from the column, followed in order by **1b**, **11b**, **10b** and **16b**.

1b: Yield: 0.26 g (0.63 mmol, 31%), red crystals. ν_{CO}(hexane)/cm^{-1} 2059 m ($A_1^{(1)}$), 1987vw (B_1), 1958sh ($A_1^{(2)}$), 1947vs (E). δ^{1}H (300.13 MHz; $CDCl_3$; Me_4Si) 7.07 (1H, d, $^3J_{4,5}$ 4.0, H4), 7.62 (1H, d, $^3J_{5,4}$ 4.0, H5), 7.13 (1H, s, H2′), 6.94 (1H, s, H4′), 7.33 (1H, s, H5′), 4.73 (2H, q, ^3J 6.5, CH_2), 1.20 (3H, t, ^3J 6.5, CH_3). δ^{13}C (75.468 MHz; $CDCl_3$; Me_4Si) 330.1 (C_{carb}), 223.5 (CO_{trans}), 216.3 (CO_{cis}), 153.0 (C2), 137.2 (C3), 130.1 (C4), 132.1 (C5), 122.4 (C2′), 130.7 (C3′), 128.1 (C4′), 125.7 (C5′), 76.4 (CH_2), 14.3 (CH_3).

2b: Yield: 0.20 g (0.48 mmol, 24%), red crystals. ν_{CO}(hexane)/cm^{-1} 2059 m ($A_1^{(1)}$), 1983vw (B_1), 1958sh ($A_1^{(2)}$), 1947vs (E). δ^{1}H (300.13 MHz; $CDCl_3$; Me_4Si) 7.71 (1H, s, H2), 8.40 (1H, s, H4), 7.47 (1H, d, $^4J_{2',5'}$ 3.2, H2′), 7.34 (1H, d, $^3J_{4',5'}$ 5.2, H4′), 7.41 (1H, dd, $^3J_{5',4'}$ 5.2 and $^4J_{5',2'}$ 3.2, H5′), 5.20 (2H, q, ^3J 7.1, CH_2), 1.69 (3H, t, ^3J 7.1, CH_3). δ^{13}C(100.613 MHz; $CDCl_3$; Me_4Si) 316.3 (C_{carb}), 223.2 (CO_{trans}), 217.1 (CO_{cis}), 129.1 (C2), 139.0 (C3), 138.9 (C4), 155.4 (C5), 120.8 (C2′), 136.0 (C3′), 126.0 (C4′), 126.8 (C5′), 76.1 (CH_2), 15.2 (CH_3)

10b: Yield: 0.40 g (0.60 mmol, 30%), purple-red crystals. ν_{CO}(hexane)/cm^{-1} 2059 m ($A_1^{(1)}$), 1984vw (B_1), 1959sh ($A_1^{(2)}$), 1948vs (E). δ^{1}H(300.13 MHz; $CDCl_3$; Me_4Si): 7.77 (2H, s, H2), 8.39 (2H, s, H4), 5.22 (4H, q, ^3J 6.7, CH_2), 1.70 (6H, t, ^3J 6.9, CH_3). δ^{13}C (75.468 MHz; $CDCl_3$; Me_4Si) 316.9 (C_{carb}), 223.1 (CO_{trans}), 217.0 (CO_{cis}), 129.4 (C2), 137.6 (C3), 138.3 (C4), 155.8 (C5), 76.2 (CH_2), 15.2 (CH_3). m/z($C_{24}H_{14}O_{12}S_2Cr_2$, 661.87 g/mol) 576.8508 (50%, $[M-H-3CO]^-$), 548.8428 (100%, $[M-H-4CO]^-$), 520.8489 (94%, $[M-H-5CO]^-$).

11b: Yield: <3%, purple-red crystals. δ^{1}H(300.13 MHz; $CDCl_3$; Me_4Si) 7.47 (2H, d, $^3J_{4,5}$ 4.4, H4), 8.18 (2H, d, $^3J_{5,4}$ 4.4, H5), 5.18 (4H, q, ^3J 7.0, CH_2), 1.70 (6H, t, ^3J 7.0, CH_3).

2.4.1.1.4. Synthesis of 2,3′-bithienyl chromium carbene complexes. 0.33 g (2.0 mmol) of 2,3′-bithiophene was dissolved in 10 mL THF, 1.9 mL (3.0 mmol) of n-BuLi and 0.66 g (3.0 mmol) of Cr(CO)$_6$ were added. Dissolved in 20.00 mL DCM, the reaction was alkylated with 0.57 g (3.0 mmol) $[Et_3O][BF_4]$. Compounds **4b**, **3b** and **5b** eluted first, followed by the biscarbene complexes **14b** and **16b**.

3b: Yield: 0.10 g (0.2 mmol, 12%), red crystals. δ^{1}H(300 MHz; $CDCl_3$; Me_4Si) 7.08 (1H, dd, H3), 7.36 (1H, dd, $^3J_{4,5}$ 4.1, H4), 7.39 (1H, dd, $^3J_{5,4}$ 4.1, H5), 7.63 (1H, br, H4′), 8.22 (1H, $^3J_{5',4'}$ 4.3, H5′), 5.17 (2H, q, ^3J 7.0, CH_2), 1.67 (3H, t, ^3J 7.0, CH_3). δ^{13}C (100.613 MHz; $CDCl_3$; Me_4Si) 312.4 (C_{carb}), 223.4 (CO_{trans}), 217.2 (CO_{cis}). 148.5 (C2), 123.1 (C3), 125.2 (C4), 127.2 (C5), 155.3 (C2′), 142.9 (C3′), 129.2 (C4′), 134.5 (C5′), 75.7 (CH_2), 15.1 (CH_3).

4b: Yield: 0.12 g (0.3 mmol, 15%), red crystals. ν_{CO}(hexane)/cm^{-1} 2059 m ($A_1^{(1)}$), 1984vw (B), 1959sh ($A_1^{(2)}$), 1948 s (E). δ^{1}H (400 MHz; $CDCl_3$; Me_4Si) 7.26 (1H, dd, $^4J_{3,5}$ 1.3, $^3J_{3,4}$ 5.0, H3), 7.08 (1H, dd, $^3J_{4,3}$ 3.7, $^3J_{4,5}$ 5.0, H4), 7.28 (1H, dd, $^3J_{5,4}$ 5.0, $^4J_{5,3}$ 1.3, H5), 7.69 (1H, d, $^4J_{2',4'}$ 1.3, H2′), 8.35 (1H, d, $^4J_{4',2'}$ 1.3, H4′), 5.20 (2H, q, ^3J7.0, CH_2), 1.69 (3H, t, ^3J 7.0, CH_3). δ^{13}C(100.613 MHz; $CDCl_3$; Me_4Si) 316.82(C_{carb}), 223.2 (CO_{trans}), 217.0 (CO_{cis}), 137.7 (C2), 124.9 (C3), 124.0 (C4), 128.0 (C5), 128.5 (C2′), 138.0 (C3′), 137.3 (C4′), 155.6 (C5′), 76.2 (CH_2), 15.2 (CH_3).

5b: Yield: 0.017 g (0.04 mmol, 2%), orange brown crystals. ν_{CO}(hexane)/cm^{-1} 2057 m ($A_1^{(1)}$), 1980sh ($A_1^{(2)}$), 1958 s (E). δ^{1}H

(400 MHz; $CDCl_3$; Me_4Si) 7.61 (1H, d, $^3J_{4,3}$ 5.1, H4), 7.37 (2H, dd, H3/4′), 7.42 (1H, dd, $^4J_{5',2'}$ 3.6, H2′), 7.60 (1H, dd, $^3J_{5',4'}$ 5.1, H5′), 5.34 (2H, q, ^3J 7.1, CH_2), 1.71 (3H, t, ^3J 7.1, CH_3).

14b: Yield: 0.35 g (0.4 mmol, 22%), brown red crystals. ν_{CO}(hexane)/cm^{-1} 2057 m ($A_1^{(1)}$), 1984vw (B_1), 1950 s (E). δ^1H(400 MHz; $CDCl_3$; Me_4Si) 7.40 (1H, d, $^3J_{3,4}$ 4.2, H3), 8.24 (1H, d, $^3J_{4,3}$ 4.2, H4), 7.89 (1H, d, $^4J_{4',2'}$ 1.3, H2′), 8.36 (1H, d, $^4J_{4',2'}$ 1.3, H4′), 5.22 (2H, q, ^3J 7.0, CH_2), 5.19 (2H, q, ^3J 7.0, CH_2), 1.70 (6H, t, ^3J 7.0, CH_3). δ^{13}C (100.613 MHz; $CDCl_3$; Me_4Si) 317.2(C-5′) (C_{carb}), 313.8(C-5) (C_{carb}), 223.3 and 223.1 (CO_{trans}), 217.1 and 216.8 (CO_{cis}), 146.3 (C2), 125.6 (C3), 142.6 (C4), 153.1 (C5), 130.6 (C2′), 136.0 (C3′), 137.1 (C4′), 156.1 (C5′), 76.6 and 76.0 (CH_2), 15.3 and 15.1 (CH_3). *m/z*($C_{24}H_{14}O_{12}S_2Cr_2$, 661.8737 g/mol), 661.8837 (14%, $[M]^-$), 633.8876 (45%, $[M{-}CO]^-$), 605.8925 (100%, $[M{-}2CO]^-$), 577.8991 (31%, $[M{-}3CO]^-$), 549.9061 (71%, $[M{-}4CO]^-$), 521.9091 (35%, $[M{-}5CO]^-$).

16b: Yield: 0.08 g (0.1 mmol, 5%), blue crystals. ν_{CO}(hexane)/cm^{-1} 2054 m ($A_1^{(1)}$), 1983vw (B_1), 1952 m ($A_1^{(2)}$), 1940vs (E). δ^1H (400 MHz; $CDCl_3$; Me_4Si) 8.18 (2H, d, $^3J_{3,4}$ 4.2, H3/H3′), 7.47 (2H, d, $^3J_{4,3}$ 4.2, H4/H4′), 5.19 (2H, q, ^3J 7.1, CH_2), 1.70 (3H, t, ^3J 7.1, CH_3). δ^{13}C(100.613 MHz; $CDCl_3$; Me_4Si) 314.3 (C_{carb}), 223.4 (CO_{trans}), 216.9 (CO_{cis}), 144.3 (C2), 141.8 (C3), 127.1 (C4), 154.3 (C5), 76.0 (CH_2), 15.2 (CH_3).

2.4.1.2. Method 2.

2.4.1.2.1. Synthesis of chromium and tungsten heterobimetallic 3,3′-bithienylene biscarbene complex. 0.75 g (4.5 mmol) of 3,3′-bithiophene was dissolved in 30 mL THF, 3.10 mL (5.0 mmol) of *n*-BuLi was added at −78 °C and the reaction mixture stirred for 30 min. Solid portions of 1.58 g (4.5 mmol) $W(CO)_6$ were then added. After 15 min of stirring, the solution was removed from the cold bath and stirred for a further 40 min at room temperature. The solution was then cooled to −78 °C and 3.10 mL (5.0 mmol) of *n*-BuLi was added and the mixture was allowed to stir for 30 min. Solid portions of 0.99 g (4.5 mmol) $Cr(CO)_6$ were then added. After 15 min of stirring, the solution was removed from the cold bath and stirred for a further 40 min at room temperature. The solvent was removed *in vacuo*, the reaction residue was dissolved in 10 mL DCM and cooled to −30 °C. 1.70 g (9.0 mmol) of $[Et_3O][BF_4]$ was dissolved in 10 mL DCM and added to the cold reaction mixture that was then allowed to rise to room temperature. The mixture was filtered through a silica gel plug with DCM and the solvent removed at a reduced pressure. Column chromatography yielded seven complexes. The monocarbene complexes (**2b**, **1b**, **2a** and **1a**) eluted first, followed by the biscarbene complexes (**13ab/ba** and **10b**).

13ab: Yield: 1.48 g (1.86 mmol, 57%), purple-red crystals. ν_{CO}(hexane)/cm^{-1} 2072w and 2064w ($A_1^{(1)}$, W), 2057 m ($A_1^{(1)}$, Cr), 1987vw (B_1, Cr), 1984vw (B_1, W), 1961sh ($A_1^{(2)}$), 1955vs (E). δ^1H (400.13 MHz; $CDCl_3$; Me_4Si): 8.04 (1H, s, H4), 7.19 (1H, dd, $^4J_{2',5'}$ 2.9 and $^4J_{2',4'}$ 1.1, H2′), 6.96 (1H, dd, $^3J_{4',5'}$ 5.0 and $^4J_{4',2'}$ 1.0, H4′), 7.36 (1H, dd, $^3J_{5',4'}$ 5.0 and $^4J_{5',2'}$ 3.0, H5′), 4.73 (2H, q, ^3J 7.0, **C2**CH_2), 5.21 (2H, q, ^3J 7.0, **C5**CH_2), 1.27 (3H, t, ^3J 7.1, **C2**CH_3) 1.70 (3H, t, ^3J 7.0, **C5**CH_3). δ^{13}C(100.613 MHz; $CDCl_3$; Me_4Si) 304.6 (C_{carb} W), 317.7 (C_{carb} Cr), 203.0 (CO_{trans} W), 196.6 (CO_{cis} W), 223.4 (CO_{trans} Cr), 216.6 (CO_{cis} Cr), 155.4 (C2), 136.1 (C3), 140.1 (C4), 155.4 (C5), 123.1 (C2′), 131.6 (C3′), 127.9 (C4′), 126.0 (C5′), 79.4 (CH_2 W), 76.4 (CH_2 Cr), 14.1 (CH_3 W). 15.1 (CH_3 Cr). *m/z*($C_{24}H_{14}O_{12}S_2WCr$, 793.88 g/mol) 624.8883 (9%, $[M{-}H{-}6CO]^-$), 596.8881 (72%, $[M{-}H{-}7CO]^-$), 568.8915 (100%, $[M{-}H{-}8CO]^-$).

13ba: Yield: 0.39 g (0.49 mmol, 15%), purple-red crystals). δ^1H (400.13 MHz; $CDCl_3$; Me_4Si): 7.97 (1H, s, H4), 7.16 (1H, dd, $^4J_{2',5'}$ 2.8 and $^4J_{2',4'}$ 1.0, H2′), 7.00 (1H, dd, $^3J_{4',5'}$ 4.9 and $^4J_{4',2'}$ 1.1, H4′), 7.38 (1H, dd, $^3J_{5',4'}$ 5.0 and $^4J_{5',2'}$ 3.0, H5′), 4.73 (2H, q, ^3J 7.0, **C2**CH_2), 5.01 (2H, q, ^3J 7.0, **C5**CH_2), 1.39 (3H, t, ^3J 7.1, **C2**CH_3) 1.68 (3H, t, ^3J 7.2, **C5**CH_3). δ^{13}C(100.613 MHz; $CDCl_3$; Me_4Si) 290.7 (C_{carb} W), 317.7 (C_{carb} Cr), 202.4 (CO_{trans} W), 197.3 (CO_{cis} W), 223.8 (CO_{trans} Cr), 215.3 (CO_{cis} Cr), n.o. (C2), n.o. (C3), 140.0 (C4), n.o. (C5), 123.2 (C2′), n.o. (C3′), 127.5 (C4′), 126.5 (C5′), 78.8 (CH_2 W), 76.4 (CH_2 Cr), 14.9 (CH_3 W). 14.6 (CH_3 Cr).

2.4.2. General procedure for the synthesis of aminocarbene complexes

2.4.2.1. Method 3. In the case of 3,3′-bithiophene the ethoxycarbene complexes were dissolved in an ethereal solution, to which an ether solution saturated with NH_3 (g) was added dropwise. The reactions are monitored by TLC and after full conversion (colour change), the aminocarbene complexes are purified by column chromatography and crystallised from DCM/hexane mixtures.

2.4.2.1.1. Synthesis of 3,3′-bithienyl tungsten aminocarbene complexes. 0.25 g (0.5 mmol) of a mixture of **1a** and **2a** was dissolved in 10 mL diethyl ether. The reaction yielded two complexes. Compound **6a** was the first to elute from the column, followed by **7a**.

6a: Yield: 0.15 g (0.29 mmol, 63%), yellow crystals. ν(hexane)/cm^{-1} ν_{as} NH_2 3452w and 3241vw (hydrogen bonding), ν_s NH_2 3338w and 3123vw (hydrogen bonding), ν_{CO} 2065 m ($A_1^{(1)}$), 1978 m (B_1), 1945 and 1930vs ($A_1^{(2)}$ and E), ν CN and δ_s NH_2 1675 m (hydrogen bonding) and 1630 m. ν(KBr)/cm^{-1} ν_{as} NH_2 3445w and 3257vw (hydrogen bonding), ν_s NH_2 3331w and 3122vw (hydrogen bonding), ν_{CO} 2064 m ($A_1^{(1)}$), 1977 m (B_1), 1931, 1924 and 1905vs ($A_1^{(2)}$ and E), ν CN and δ_s NH_2 1637 m. δ^1H(300.13 MHz; $CDCl_3$; Me_4Si): 8.51 and 8.21 (2H, br s, NH_2), 7.13 (1H, d, $^3J_{4,5}$ 5.1, H4), 7.67 (1H, d, $^3J_{5,4}$ 5.1, H5), 7.33 (1H, dd, $^4J_{2',5'\text{ and }2',4'}$ 3.0 and 1.3, H2′), 7.09 (1H, dd, $^3J_{4',5'}$ 5.0 and $^4J_{4',2'}$ 1.3, H4′), 7.45 (1H, dd, $^3J_{5',4'}$ 5.0 and $^4J_{5',2'}$ 3.0, H5′). δ^{13}C(75.468 MHz; $CDCl_3$; Me_4Si): 247.3 (C_{carb}), 202.5 (CO_{trans}), 198.4 (CO_{cis}), 150.9 (C2), 135.3 (C3), 131.4 (C4), 132.7 (C5), 124.0 (C2′), 130.5 (C3′), 127.7 (C4′), 127.5 (C5′). *m/z*($C_{14}H_7O_5S_2NW$, 516.93 g/mol) 515.9099 (3%, $[M{-}H]^-$), 431.9154 (89%, $[M{-}H{-}3CO]^-$), 375.9400 (100%, $[M{-}H{-}5CO]^-$).

7a: Yield: 0.08 g (0.15 mmol, 33%), bright yellow crystals. ν (DCM)/cm^{-1} ν_{as} NH_2 3451w and 3255vw (hydrogen bonding), ν_s NH_2 3333w and 3118vw (hydrogen bonding), ν_{CO} 2073 m ($A_1^{(1)}$), 1983w (B_1), 1933vs ($A_1^{(2)}$ and E), ν CN and δ_s NH_2 1641 m. ν(KBr)/cm^{-1} ν_{as} NH_2 3455w and 3258vw (hydrogen bonding), ν_s NH_2 3332w and 3112vw (hydrogen bonding), ν_{CO} 2062 m ($A_1^{(1)}$), 1980 m and 1980 m (B_1), 1952, 1904 and 1887vs ($A_1^{(2)}$ and E), ν CN and δ_s NH_2 1640 m. δ^1H(300.13 MHz; $CDCl_3$; Me_4Si): 8.61 and 8.16 (2H, br s, NH_2), 7.73 (1H, d, $^4J_{2,4}$ 1.3, H2), 7.83 (1H, d, $^4J_{4,2}$ 1.4, H4), 7.44 (1H, dd, $^4J_{2',5'\text{ and }2',4'}$ 2.9 and 1.3, H2′), 7.32 (1H, dd, $^3J_{4',5'}$ 5.0 and $^4J_{4',2'}$ 1.3, H4′), 7.41 (1H, dd, $^3J_{5',4'}$ 5.0 and $^4J_{5',2'}$ 3.0, H5′). δ^{13}C(75.468 MHz; $CDCl_3$; Me_4Si): 244.5 (C_{carb}), 202.3 (CO_{trans}), 198.4 (CO_{cis}), 125.9 (C2), 139.0 (C3), 130.6 (C4), 153.9 (C5), 121.1 (C2′), 135.8 (C3′), 126.9 (C4′), 127.0 (C5′). *m/z*($C_{14}H_7O_5S_2NW$, 516.93 g/mol) 515.9066 (4%, $[M{-}H]^-$), 431.9137 (17%, $[M{-}H{-}3CO]^-$), 375.9373 (100%, $[M{-}H{-}5CO]^-$).

2.4.2.1.2. Synthesis of 3,3′-bithienyl chromium aminocarbene complexes. 0.25 g (0.6 mmol) of a mixture of **1b** and **2b** was used, yielding two complexes. Compound **6b** was the first to elute from the column, followed by **7b**.

6b: Yield: 0.13 g (0.3 mmol, 54%), yellow crystals. ν(hexane)/cm^{-1} ν_{as} NH_2 3457w and 3241vw (hydrogen bonding), ν_s NH_2 3333w and 3122 m (hydrogen bonding), ν_{CO} 2058 m ($A_1^{(1)}$), n.o. (B_1), 1948, 1944 and 1934vs ($A_1^{(2)}$ and E), ν CN and δ_s NH_2 1729w (hydrogen bonding), 1675 m (hydrogen bonding) and 1629 m. ν (KBr)/cm^{-1} ν_{as} NH2 3442w and 3253vw (hydrogen bonding), ν_s NH_2 3331w and 3119 m (hydrogen bonding), ν_{CO} 2072 m and 2055 m ($A_1^{(1)}$), n.o. (B_1), 1931 and 1893vs ($A_1^{(2)}$ and E), ν CN and δ_s NH_2 1715w (hydrogen bonding) and 1655 m. δ^1H(400.13 MHz; $CDCl_3$; Me_4Si): 8.47 and 8.12 (2H, br s, NH_2), 7.06 (2H, s br, H4 and H4′), 7.61 (1H, s, H5), 7.28 (1H, s, H2′), 7.41 (1H, s, H5′). δ^{13}C (100.613 MHz; $CDCl_3$; Me_4Si): 273.0 (C_{carb}), 222.5 (CO_{trans}), 217.1 (CO_{cis}), 149.6 (C2), 135.2 (C3), 130.6 (C4), 131.7 (C5), 123.8 (C2′), 129.1 (C3′), 127.8 (C4′), 127.2 (C5′). *m/z*($C_{14}H_7O_5S_2NCr$, 384.92 g/mol) 383.9025 (2%, $[M{-}H]^-$), 327.9077 (40%, $[M{-}H{-}2CO]^-$), 243.9217 (100%, $[M{-}H{-}5CO]^-$).

7b: Yield: 0.10 g (0.26 mmol, 42%), bright yellow crystals. ν (DCM)/cm^{-1} ν_{as} NH_2 3453 m and 3255w (hydrogen bonding), ν_s NH_2 3331w and 3120vw (hydrogen bonding), ν_{CO} 2057 m ($A_1^{(1)}$), 1984w (B_1), 1936vs ($A_1^{(2)}$ and E), ν CN and δ_s NH_2 1635 m. ν(KBr)/cm^{-1} ν_{as} NH_2 3441 m and 3255w (hydrogen bonding), ν_s NH_2 3329w and 3122vw (hydrogen bonding), ν_{CO} 2053 m ($A_1^{(1)}$), 1977w (B_1), 1958, 1928 and 1910vs ($A_1^{(2)}$ and E), ν CN and δ_s NH_2 1652 m. δ^1H(400.13 MHz; $CDCl_3$; Me_4Si) :8.31 (2H, br s, NH_2), 7.64 (1H, s, H2), 7.85 (1H, s, H4), 7.45 (1H, s, H2′), 7.32 (1H, d, $^3J_{4',5'}$ 5.2, H4′), 7.41 (1H, d, $^3J_{5',4'}$ 5.2, H5′). δ^{13}C(100.613 MHz; $CDCl_3$; Me_4Si): 269.1 (C_{carb}), 222.5 (CO_{trans}), 217.4 (CO_{cis}), 125.6 (C2), 138.9 (C3), 130.6 (C4), 151.8 (C5), 121.0 (C2′), 135.8 (C3′), 126.0 (C4′), 126.8 (C5′). *m/z*($C_{14}H_7O_5S_2NCr$, 384.92 g/mol) 383.9034 (4%, $[M{-}H]^-$), 327.9134 (36%, $[M{-}H{-}2CO]^-$), 243.9295 (100%, $[M{-}H{-}5CO]^-$).

2.4.2.2. Method 4 [15]. In the case of 2,3′-bithiophene, the ethoxycarbene complexes were dissolved in THF and solid dimethylamine hydrochloride and NaOH pellets were added, while stirring vigorously. Dropwise addition of distilled water dissolved the solids and generated dimethylamine *in situ*. Two layers were observed and the organic phase was washed with dried diethyl-ether and the combined diethyl ether fractions filtered over anhydrous $MgSO_4$ and silica gel. Solvents were removed under reduced pressure and purification was done with column chromatography.

2.4.2.2.1. Synthesis of 2,3′-bithienyl tungsten aminocarbene complexes. 0.44 g (0.8 mmol) of an inseparable mixture of **3a** and **4a** was dissolved in 15 mL THF. To the reaction mixture, dimethylamine hydrochloride (0.10 g, 1.2 mmol) and sodium hydroxide (0.05 g, 1.2 mmol) were added. Compound **9a** was the first to elute from the column, followed by **8a**.

8a: Yield: 0.22 g (0.4 mmol, 51%), yellow crystals. ν_{CO}(dichloromethane)/cm^{-1} 2064 m ($A_1^{(1)}$), 1975w (B_1), 1939 s (E). δ^1H(400 MHz; $CDCl_3$; Me_4Si) 7.06 (2H, dd, H3/4), 7.29 (1H, dd, $J = {}^3J_{5,4}$ 5.1, H5), 7.20 (1H, d, $^3J_{4',5'}$ 5.1, H4′), 7.32 (1H, d, $^3J_{5',4'}$ 5.1, H5′), 3.93 (3H, s, CH_3), 3.09 (3H, s, CH_3). δ^{13}C(100.613 MHz; $CDCl_3$; Me_4Si), 251.0 (C_{carb}), 203.3 (CO_{trans}), 197.9 (CO_{cis}), 123.3 (C2), 124.8 (C3), 124.2 (C4), 125.4 (C5), 148.3 (C2′), 137.1 (C3′), 127.3 (C4′), 127.6 (C5′), 53.6, 44.6 (CH_3).

9a: Yield: 0.09 g (0.2 mmol, 20%), yellow crystals. ν_{CO}(dichloromethane)/cm^{-1} 2064 m ($A_1^{(1)}$), 1975w (B_1), 1939 s (E). δ^1H(400 MHz; $CDCl_3$; Me_4Si) 7.18 (1H, dd, $^3J_{3,4}$ 3.6, $^3J_{3,5}$ 1.1, H3), 7.04 (1H, dd, $^3J_{4,5}$ 5.1, $^3J_{4,3}$ 3.6, H4), 7.23 (1H, dd, $^3J_{5,4}$ 5.1, $^4J_{5,3}$ 1.1, H5), 6.79 (1H, d, $^4J_{2',4'}$ 1.4, H2′), 7.32 (1H, d, $^3J_{4',2'}$ 1.4, H4′), 3.29 (3H, s, CH_3), 3.94 (3H, s, CH_3). δ^{13}C(100.613 MHz; $CDCl_3$; Me_4Si), 250.4 (C_{carb}), 203.7 (CO_{trans}), 198.2 (CO_{cis}), 138.4 (C2), 117.7 (C3), 123.6 (C4), 127.8 (C5), 117.9 (C2′), 135.3 (C3′), 124.3 (C4′), 154.5 (C5′), 53.9 (CH_3), 45.2 (CH_3).

2.4.2.2.2. Synthesis of 2,3′-bithienylene tungsten bis-aminocarbene complex. The same procedure as described for the amino-monocarbene complexes was performed. 0.74 g (0.8 mmol) of **14a** was used.

20a C5T2-C5′T3′: Yield: 0.55 g (0.60 mmol, 75%), yellow crystals. ν_{CO}(dichloromethane)/cm^{-1} 2064 m ($A_1^{(1)}$), 1966 m (B), 1954vw ($A_1^{(2)}$), 1936 s (E). δ^1H(400 MHz; $CDCl_3$; Me_4Si) 6.50 (1H, d, $^3J_{3,4}$ 3.7, H3), 7.07 (1H, d, $^3J_{4,3}$ 3.7, H4), 6.76 (1H, d, $^4J_{2',4'}$ 1.4, H2′), 7.29 (1H, d, $^4J_{4',2'}$ 1.4, H4′), 3.95 (3H, s, CH_3), 3.93 (3H, s, CH_3), 3.30 (6H, s, CH_3). δ^{13}C(100.613 MHz; $CDCl_3$; Me_4Si), 249.8 (C-5) (C_{carb}), 250.0 (C-5′) (C_{carb}), 203.7 and 203.6 (CO_{trans}), 198.2 and 198.2 (CO_{cis}), 137.6 (C2), 117.4 (C3), 123.3 (C4), 152.4(C5), 118.1 (C2′), 134.3 (C3′), 119.9 (C4′), 154.7 (C5′), 53.9 (CH_3), 45.3 and 45.3 (CH_3).

3. Results and discussion

3.1. Synthesis and characterization of monocarbene complexes

The method of synthesis used was the classical Fischer method of deprotonation by an organolithium base, reaction with a metal carbonyl and subsequent alkylation of the metal acylate to afford the neutral carbene complexes [19]. In this study, reactions were performed at low temperatures in THF to try and discriminate between the different α-active sites and study novel products that form. Preliminary experiments with varying mole ratios of reagents indicated that the full scope of reaction products could be optimised by using 1.5 mole quantities of butyl lithium and metal carbonyl for each mole equivalent bithienyl precursor, both mono- and biscarbene complexes form in the same reaction. If 1 equivalent of butyl lithium/metal carbonyl is employed, the yields of the biscarbene complexes are reduced but their formation is still observed, implying incomplete reaction of the starting bithienyl precursor. In addition, the ratio of isomeric monocarbene complexes formed, remains approximately constant. Increasing the mole quantities of base and metal precursor employed to more than 1.5 mole quantities do not result in higher yields of the multinuclear complexes, and the reaction still yields a complicated mixture of mono- to multicarbene complexes. However, significantly more decomposition products are observed to form. Two methods of preparation for the carbene complexes were used for 3,3′-bithienyl. Method 1 (Scheme 1) involves the general procedure, while Method 2 is a modified version where reagents are added in two separate sequential steps (*vide infra*). The complexes obtained are numbered consecutively to indicate the different classes obtained; namely the ethoxy monocarbene complexes, followed by the amino monocarbene complexes, and then the ethoxy and amino biscarbene complexes, respectively. Only the first procedure was used for the 2,3′-bithienyl substrate. Isolation and purification of monocarbene complexes proved non-trivial and in some instances pure compounds could only be obtained after repeated re-crystallisation of fractions collected from the silica columns. This was applied to separate **1** from **2** and **3** from **4** (see Figs. S14–S17 in Supplementary data). Yields recorded are obtained by mass determinations of either pure compounds or of crude products obtained from fractions collected after column chromatography. In the case of mixtures peak intensities from the ^{1}H NMR spectral data were used to discriminate between products and find product ratios. For the monocarbene complexes of 3,3′-bithienyl, two classes of monocarbene complexes were isolated in very similar yields, indicating that the positions **C2T3-T3′** (**1a/b**) and **C5T3-T3′** (**2a/b**) are most reactive. These complexes represent reactions of both available α-positions and correlate well with the favoured positions indicated by molecular orbital and activation energy calculations (Fig. 2). The correlation between site activation and products isolated for 2,3′-bithienyl is in good agreement with the lower activation energies shown. Higher yields were obtained for the active sites on the T3′ ring, **T2-C2′T3′** (**3a/b**) and **T2-C5′T3′** (**4a/b**). The third and last active α-position on the 2,3′-bithienyl ring is represented by the tungsten analogue, **C5T2-T3′** (**5a**) isolated in reasonable yield; whereas only small amounts of the chromium complex **5b** formed. Notably no monocarbene complexes, with the carbene carbon in a β-position, were isolated while using *n*-BuLi. This is in line with our previous studies showing that lithium–halogen exchange is a requirement for β-carbon lithiation under the reaction conditions employed [12,19].

Replacing an ethoxy substituent with an amino substituent has a significant effect on the electronic properties of Fischer carbene complexes and especially affects the carbene carbon [20].

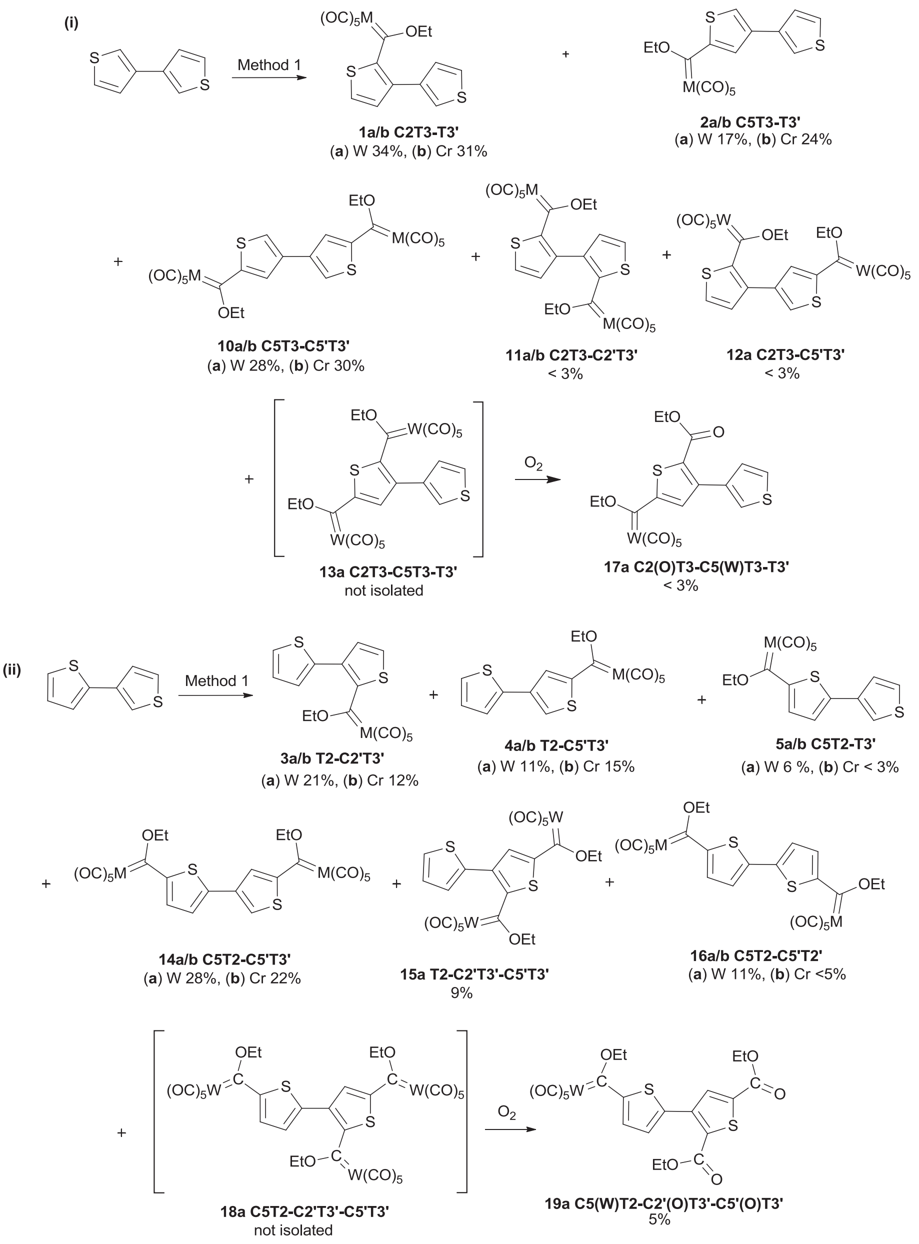

Scheme 1. Synthesis of carbene complexes from (i) 3,3′-bithienyl and (ii) 2,3′-bithienyl substrates.**Method 1**: 1.5 mole quantities of *n*-BuLi, $M(CO)_6$ in THF and $[Et_3O][BF_4]$ in DCM. Partial oxidation of the biscarbene complex (**13a**) and an unstable triscarbene complex, **C5T2-C2′T3′-C5′T3′** (**18a**)**,** to give the monocarbene complexes **C2(O)T3-C5(W)T3-T3′** (**17a**) and **C5(W)T2-C2′(O)T3′-C5′(O)T3′** (**19a**), respectively.

Selected monoethoxycarbene complexes with 3,3′-bithienyl and 2,3′-bithienyl backbones were aminolysed to give the monoaminocarbene complexes shown in Scheme 2. In the case of 3,3′-bithienyl, the monoethoxycarbene complexes were dissolved in an ethereal solution, to which an ether solution saturated with NH_3 (g) was added dropwise until the solution changed colour from red to yellow (indicating quantitative conversion into aminocarbenes, Method 3).

The challenge to separate the intractable mixture of **3a** and **4a** (*vide supra*), was addressed by a simple method to prepare dialkylamino- rather than aminocarbene complexes. The mixture of **3a** and **4a** was dissolved in THF and solid dimethylamine hydrochloride and NaOH pellets were added, while stirring vigorously (Method 4).

Dropwise addition of water dissolved the solids and generated dimethylamine *in situ*, which aminolysed the ethoxycarbene complexes [15]. Reactions were monitored by TLC and after full conversion, the aminocarbene complexes were purified by column chromatography and crystallised from dichloromethane (DCM)/hexane mixtures.

The monocarbene complexes were characterised by NMR and IR spectroscopy, as well as mass spectrometry and X-ray crystal structure determinations. The monocarbene complexes display the typical IR pattern of four bands (C_{4v} symmetry for $M(CO)_5$ fragment) in the carbonyl region of their IR spectra [21]. Molecular structures were confirmed by assignment of chemical shifts and associated coupling constants (see Table 2, Experimental section and Supplementary data). A Fischer carbene carbon attached to a dithienyl substituent has a significant impact on the chemical shifts of the thienyl protons in their ^1H NMR spectra. The proton resonance of the thienyl position adjacent to the carbene carbon is most affected and shifted significantly downfield due to the strong electron-withdrawing properties of the metalcarbonyl-carbene moiety (Fig. 3). In the case of the thienyl which is substituted

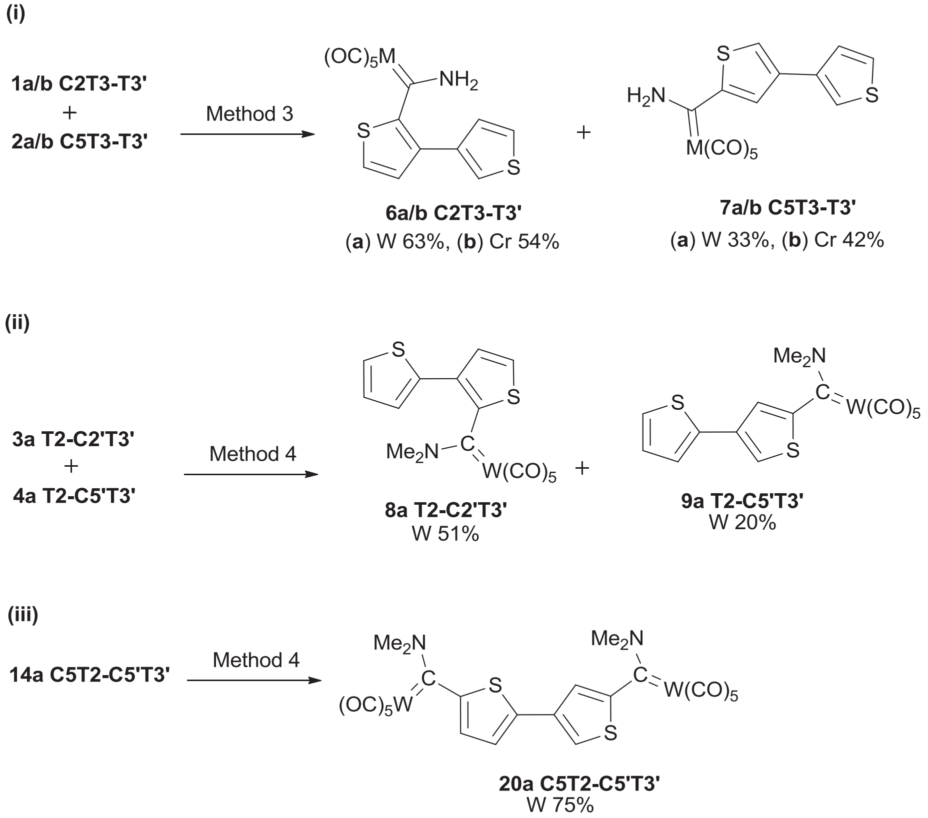

Scheme 2. Aminolysis of mono-ethoxycarbene complexes **Method 3**: Adding an ether solution saturated with $NH_3(g)$; **Method 4**: The *in situ* generation of $NHMe_2$ from $[NH_2Me_2]Cl$ and NaOH in an aqueous THF solution.

at the 3-position (T3), the carbene carbon can be found at either the C2-position (**1** or **3**, inside of T3 ring) or at the C5-position or outside α-position (**2** or **4**). The ^{1}H NMR chemical shifts of the protons of the second thienyl ring (without a carbene substituent) in **1** and **3**, are shifted significantly upfield compared to the corresponding protons of **2** and **4** (Fig. 3).

As for **2** and **4**, **1** and **3** display chemical shifts of the methylene protons of the ethoxy substituents of the carbene complexes that are almost the same, emphasizing the important differences in electronic features of inside vs outside carbene fragments in bithienyl carbene complexes. The difference between the chemical shifts of the ethoxy methylene protons in **2a** and **2b** is metal dependent ($\Delta\delta = 0.19$), but this is not the case for the carbene moiety on the inside of the bithienyl in **1a** and **1b** ($\Delta\delta = 0.02$). We ascribe this to the ethoxy substituent of the carbene carbon, in **1**, playing a smaller role to stabilise the carbene carbon which is compensated for by inter-ring electron delocalization. Also, a similar trend is observed for the methyl protons of the ethoxy substituent.

Replacing an ethoxy with an amino substituent (Scheme 2) has a significant effect on the chemical shifts in the ^{1}H and ^{13}C NMR spectra of the complexes, especially the carbene carbon and the proton resonances of the adjacent thienyl carbon are affected. The chemical shifts for the carbene carbons of aminocarbene complexes with the same metal and thienylene substituent is lowered by *ca* 50 ppm when compared to an analogous ethoxycarbene complexes in their ^{13}C NMR spectra [22]. The superior stabilization of carbene carbons by N-donor heteroatoms compared to oxygen in Fischer carbene complexes is well-known, and demonstrated by an upfield chemical shift value of the hydrogen atom adjacent to the carbene substituent on the thienyl ring in **7a** (7.83 ppm) compared to **2a** (8.30 ppm) and **9a** (7.32 ppm) compared to **4a** (8.25 ppm). Other thienyl protons are little affected. By contrast, the dithienyl substituent plays a much smaller role in stabilising the electrophilic carbene carbon in the case of aminolysed complexes compared to ethoxycarbene complexes. The molecular structures and atom numbering are displayed in Fig. 4 for representative examples **1a**, **2a**, **4a**, **7a** and **8a**; and selected bond properties are listed in Table 3.

Diffraction structural data of the analogous chromium complexes **2b** and **4b** are found in Fig. S1 and Table S1, Supplementary data. The planar single crystal structures of 3,3′-bithienyl and 2,3′-bithienyl were first determined by Visser et al. [4], but an improved refined structure by Costa et al. [23] displayed a planar 3,3′-bithiophene structure indicating inter-ring electron delocalization (torsion angle around the inter-ring bond is 180.0(1)°). The complexes with the carbene moiety in the C5-position represent a more linear (open) arrangement for the dithienyl and ethoxy substituents of the carbene ligand. In **2a**, **2b**, **4a** and **4b** the ethoxy substituents point towards the sulphur atom of the adjacent thienyl ring, which is the electronically favoured conformation [6,7,19]. However for the aminolysed complex (**7a**), the nitrogen atom is on the opposite side of the thienylene sulphur atom; emphasizing the electronic and steric differences between an amino- and an ethoxycarbene substituent in Fischer carbene complexes. In **1a**, the second thienyl ring is twisted out of the bithiophene plane due to steric congestion and is found pointing towards the plane of the second thienyl ring. By contrast, in **8a** the dimethylaminocarbene substituent deviates from sp^3-hybridisation (125°, 123° and 112°, Table 3) to approach more closely sp^2-hybridisation as expected for aminocarbenes where the C═N double bond character results from the significant carbene-heteroatom stabilization. As a result the two hydrogen or two methyl substituents are in different electronic environments displaying either two separate or a broad signal for the chemical shifts in the ^{1}H NMR spectra of **6**, **7**,

Table 2
Selected chemical shifts (δ) of the monocarbene complexes (^1H NMR/^{13}C NMR).

Complex	H/C2	H/C3	H/C4	H/C5	H/C2′	H/C3′	H/C4′	H/C5′	C_{carb}	C_{CO}[a]	OEt[b]/NR_2
1a (^1H)/(^{13}C)	/156.8	/137.8	7.12/131.6	7.71/134.1	7.15/122.4	/133.5	6.94/128.5	7.32/125.2	/298.6	/202.6, 197.4	4.71, 1.14/79.0, 14.0
1b	/153.0	/137.2	7.07/130.1	7.62/132.1	7.13/122.4	/130.7	6.94/128.1	7.33/125.7	/330.1	/223.5, 216.3	4.73, 1.20/76.4, 14.3
2a	7.83/130.2	/139.2	8.30/138.9	/158.5	7.46/120.8	136.0	7.33/126.0	7.41/126.8	/290.6	/202.4, 197.6	5.01, 1.68/78.6, 15.0
2b	7.71/129.1	/139.0	8.40/138.9	/155.4	7.47/120.8	/136.0	7.34/126.0	7.41/126.8	/316.3	/223.2, 217.1	5.20, 1.69/76.1, 15.2
3a	/149.5	6.97/123.1	7.03/125.1	7.31/127.2	/155.2	/143.7	7.16/131.4	7.64/134.6	/288.9	/202.5, 197.2	4.76, 1.67/78.1, 14.1
3b	/148.5	7.08/123.1	7.36/125.2	7.39/127.3	/155.3	/142.9	7.63/129.2	8.22/134.5	/312.4	/223.4, 217.2	5.17, 1.67/75.5, 15.1
4a	/137.6	7.26/124.0	7.08/125.0	7.28/128.0	7.82/129.6	/138.2	8.25/137.2	/158.6	/290.7	/202.4, 197.5	5.01, 1.68/78.7, 15.0
4b	/137.7	7.26/124.9	7.08/124.0	7.28/128.0	7.69/128.5	/138.0	8.35/137.3	/155.6	/316.8	/223.2, 217.0	5.20, 1.69/76.2, 15.2
5a		7.33/128.7	7.73/132.3	/147.1	7.39/133.3	/141.5	7.57/122.9	7.35/132.7	/288.4	/202.4	5.07, 1.67/77.9, 15.1
5b[c]			7.61		7.42	7.37	7.37	7.60			5.34, 1.71
6a	/150.9	/135.3	7.13/131.4	7.67/132.7	7.33/124.0	/130.5	7.09/127.7	7.45/127.5	/247.3	/202.5, 198.4	8.51, 8.21/
6b	/149.6	/135.2	7.06/130.6	7.61/131.7	7.28/123.8	/129.1	7.06/127.8	7.41/127.2	/273.0	/222.5, 217.1	8.47, 8.12/
7a	7.73/125.9	/139.0	7.83/130.6	/153.9	7.44/121.1	/135.8	7.32/126.9	7.41/127.0	/244.5	/202.3, 198.4	8.61, 8.16/
7b	7.64/125.6	/138.9	7.85/130.6	/151.8	7.45/121.0	/135.8	7.32/126.0	7.41/126.8	/269.1	/222.5, 217.4	8.31(br)/
8a	/123.3	7.06/124.8	7.06/124.2	7.29/125.4	/148.3	/137.1	7.20/127.3	7.32/127.6	/251.0	/203.3, 197.9	3.93, 3.09/53.6, 44.6
9a	/138.4	7.18/117.7	7.04/123.6	7.23/127.8	6.79/117.9	/135.3	7.32/124.3	/154.5	/250.4	/203.7, 198.2	3.94, 3.29/53.9, 45.2

[a] Carbon chemical shifts for the metalcarbonyls are reported with the first value being the chemical shift of the carbonyl *trans* to the carbene carbon, and the second the chemical shift of the carbonyls *cis* to the carbene carbon.

[b] Carbon chemical shifts for the ethoxy fragment are reported with the first value being the chemical shift of the methylene group, and the second the chemical shift of the methyl group.

[c] Sample size too small to record ^{13}C NMR spectra.

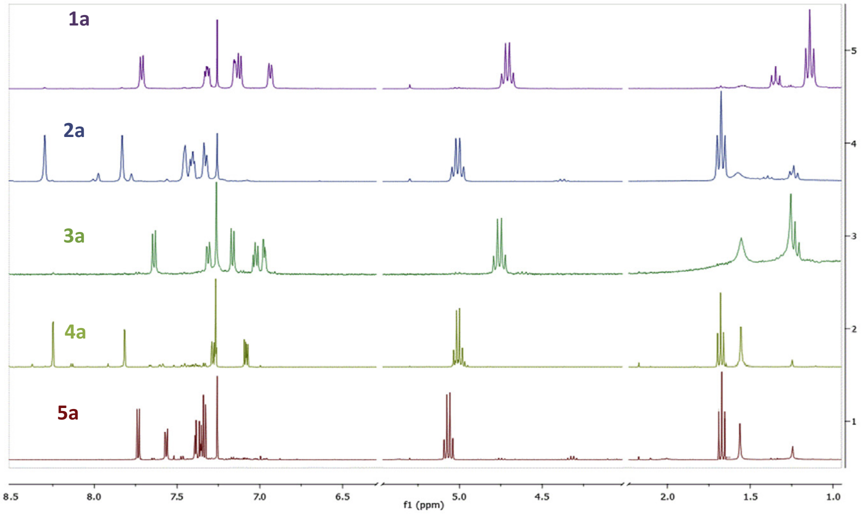

Fig. 3. ^1H NMR spectra showing chemical shift patterns of **1a**–**5a**.

8a and **9a**. The first thienyl ring is rotated to take up a position perpendicular to the carbene-amine plane (torsion angle N-C_{carb}-C_{ipso}-C_T = 88.9(4)°), ascribed to intramolecular hydrogen bonding between the nitrogen lone pair and a hydrogen in the α-position of the second thiophene ring (CH···NMe_2 2.503(4) Å). Thus, for **2a**, **4a** and **7a**, with the carbene-carrying thiophene on the outside position (C5-position), the bithienyl backbone is expected to be more planar as the second thienyl ring points away from the other two carbene substituents with minimum steric interaction between the carbene substituents (see Table 3, C_T-C_{ipso}-C'_{ipso}-C'_T torsion angles). This is not the case with the carbene-metal unit on the inside (C2-position, **1a** and **8a**), which display a greater crowded arrangement between the substituents leading to significant congestion and resulting in more restricted rotation around the thienyl-thienyl C—C bond. When attached to a carbene ligand in a metal carbonyl complex, the torsion angle defined by the thienyl-thienyl inter-ring bond varies between 0° and 90° for all the complexes and is illustrated by the extreme examples of the carbene ligands of **1a** with **7a** (Fig. S2, Supplementary data). A deviation from planarity of the bithienyl moiety is indicative of less inter-ring electron delocalization and follows the order: **7a** < **8a** < **2a** < **4a** < **1a**, for the tungsten complexes. Rotation around the inter-ring bond of the thiophene rings generates two averaged positions for the sulphur atom of the second thiophene ring, observed for all of the monocarbene structures. The W-C_{carb} distances in the complexes are longer compared to the same distance in the corresponding tungsten monocarbene complexes of thienyl (2.208(2) Å) or 2,2′-bithienyl (2.205(7) Å) [7].

3.2. Synthesis and characterization of biscarbene complexes

The biscarbene complexes of the bithienyl substrates are obtained from the same reaction mixture and collected from the column after elution of the monocarbene complexes (Scheme 1). By increasing the polarity, biscarbene complexes are separated and subsequently characterised. Although electronically favoured,

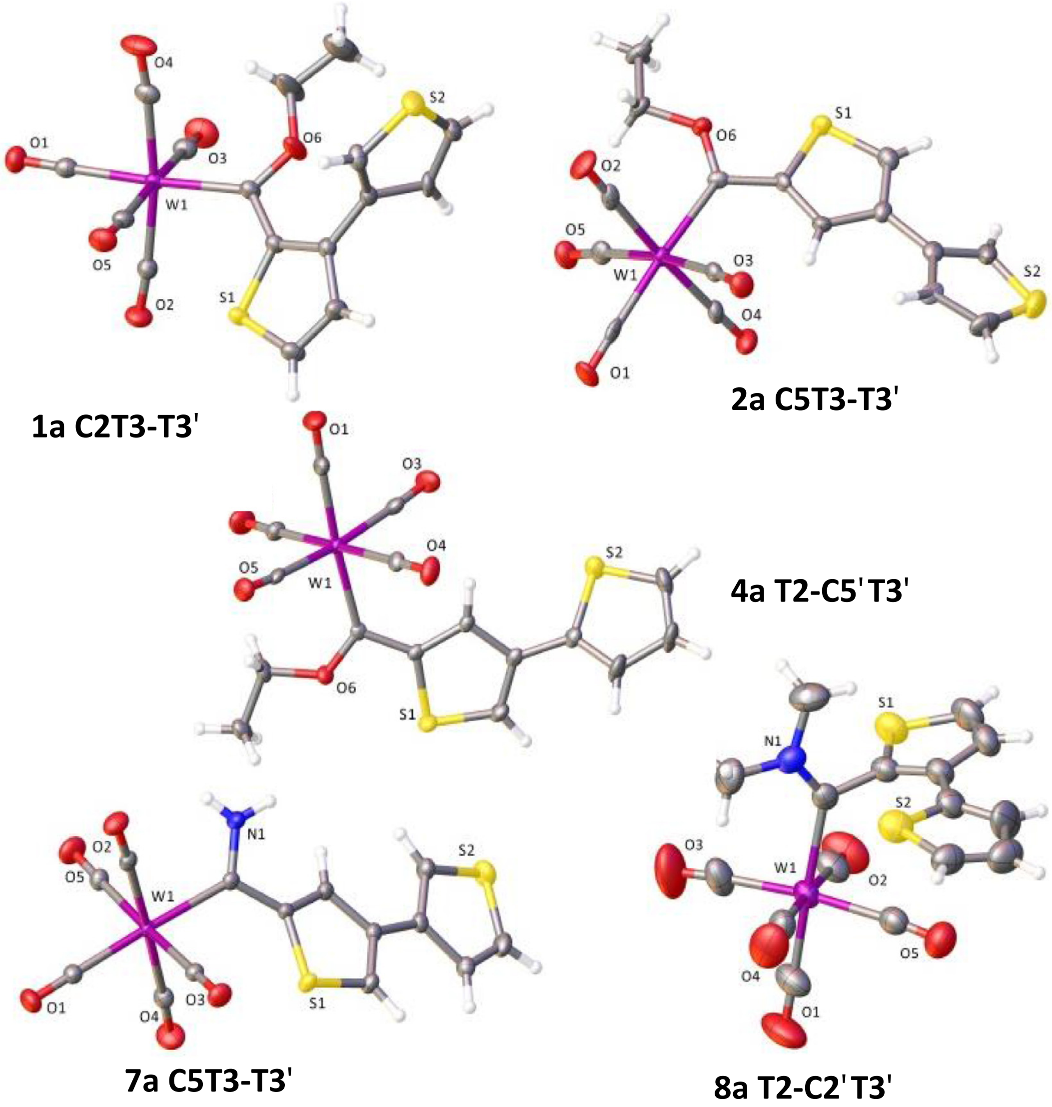

Fig. 4. The molecular structures with atom numbering of **1a**, **2a**, **4a**, **7a** and **8a** with atomic displacement ellipsoids shown at the 50% probability level.

the biscarbene complexes with the carbene substituents unit on the 'inside' are only obtained in low yield. These complexes display inter-ring electron delocalization by π-resonance effects but have large groups in close proximity and hence represent sterically less favoured isomers. The major biscarbene product in the case of 3,3′-bithienyl is **C5T3-C5′T3′** (**10a**/**b**) (outside-outside), avoiding the steric more congested and favoured 2-position, However, low yields of the calculated, expected (inside-inside) **C2T3-C2′T3′** (**11a**) isomers as well as **C2T3-C5′T3′** (**12a**) (inside-outside) isomers form, but could only be indicated by their NMR spectra; the latter only in a mixture with **10a** (Table 4, Figs. S37 and S38, Supplementary data).

Scheme 1 also illustrates the formation of a biscarbene complex **C2T3-C5T3-T3′**, **13a**, with both the carbene substituents on the same thienyl ring of 3,3′-bithienyl. The presence of **13a** in the reaction mixture is confirmed by the formation of a partially oxidised tungsten monocarbene complex **C2(0)T3-C5(W)T3-T3′**, **17a**. Chromium carbonyl carbene complexes are even more reactive compared to their tungsten analogues and neither the corresponding **13b** nor **17b** are observed. However the formation of an analogous biscarbene complex **T2-C2′T3′-C5′T3′**, **15a**, in reasonable yield is found during the reaction with lithiated 2,3′-bithienyl (*vide infra*). The heterobimetallic biscarbene complexes,**C2(W)T3-C5(Cr)T3-T3′ 13ab** and **C2(Cr)T3-C5(W)T3-T3′, 13ba,** were prepared in high yields by using Method 2 (Scheme 3). This was an extension of our previous work of preparing α,α′-thiophene mixed metal biscarbene complexes and the method to prepare the mixed metal biscarbene complex was adapted from the method used to prepare analogous heterobimetallic carbene complexes of bithiophene [2,6] and 2,5-furan [24]. The C5,C5′-mixed W, Cr biscarbene complex of 2,2′-bithienyl was synthesized to test such complexes for non-linear optical properties [25].

The stepwise lithiation method allows the introduction of two different metal carbonyls. The two isomers **13ab** and **13ba** proved to be inseparable by column chromatography and were collected as a mixture in the same band.

Furthermore, the biscarbene complexes **13ab** and **13ba** co-crystallises as two isomeric complexes in a single crystal. In the case of the major product **13ab**, the first monolithium tungsten acylmetallate forms at the C2-position, followed by the second lithium chromium acylmetallate at the C5-position. The heterometal biscarbene complexes **13ab** and **13ba** are more stable than **13a**. The

Table 3
Selected bond lengths (Å), bond angles (°) and torsion angles (°) of the structures of **1a**, **2a**, **2b**, **4a**, **4b**, **7a** and **8a**.

	1a	**2a**	**4a**	**7a**	**8a**
Bond lengths (Å)					
W–C_{carb}	2.2209(18)	2.216(6)	2.189(3)	2.2214(19)	2.254(3)
C_{carb}–C_{ipso}	1.458(2)	1.449(9)	1.458(4)	1.464(3)	1.489(5)
C_{carb}–O/N	1.318(2)	1.315(7)	1.331(3)	1.312(3)	1.310(4)
C2–C3	1.397(2)	1.379(9)	1.369(4)	1.377(3)	1.378(5)
C3–C4	1.411(2)	1.416(9)	1.414(4)	1.417(3)	1.430(5)
C4–C5	1.366(3)	1.372(9)	1.382(4)	1.375(3)	1.333(5)
C′2–C′3	1.443(7)	1.38(2)	1.336(9)	1.379(3)	1.326(12)
C′3–C′4	1.449(11)	1.44(2)	1.446(15)	1.438(3)	1.488(19)
C′4–C′5	1.405(17)	1.36(4)	1.360(7)	1.361(8)	1.331(9)
C—$C'_{interring}$	1.477(2)	1.478(9)	1.475(5)	1.469(3)	1.444(5)
Bond angles (°)					
C_{ipso}–C_{Carb}–O/N	106.01(16)	106.6(5)	105.3(2)	111.45(18)	114.0(3)
C_{ipso}–C_{Carb}–W	125.48(12)	124.3(4)	125.10(18)	125.84(13)	115.9(2)
W–C_{Carb}–O/N	128.44(13)	128.9(4)	129.59(18)	122.67(15)	130.1(2)
Torsion angles (°)					
W–C_{carb}–C_{ipso}–C_T[a]	160.68(15)	−11.0(10)	−5.6(4)	145.28(18)	−90.6(4)
O/N–C_{carb}–C_{ipso}–C_T	16.5(3)	173.1(6)	175.3(2)	−32.5(3)	88.9(4)
C_X–O/N–C_{carb}–W	−3.8(4)	4.7(9)	3.5(4)		177.5(3)
					−2.1(5)
C_T–C_{ipso}–C'_{ipso}–C'_T	89.0(3)	−23.2(11)	−38.0(11)	-173.1(3)	160.0(13)
	80.2(5)	−25.2(11)	140.0(11)	-174.9(5)	18.3(14)

[a] C_T = Thienyl carbon atom.

occurrence of both carbenes on one thiophene ring is made possible by the anionic protection of the first acylmetallate [26], allowing communication through linear conjugation between C2 and C5. In a control experiment, using method 2 with thiophene as substrate, an even more stable mixed metal (W/Cr) biscarbene complex of thiophene, **21ab** and **21ba** are obtained in high yields [27]. The stability of the mixed and homometal bis- and monocarbene complexes against oxidation, follows the order: **2a/b** > **1a/b** $\gg$ **21ab/ba** > **13ab/ba** > **15a** > **13a**. The major biscarbene product in the case of 2,3′-bithienyl is again the outside-outside isomer, **C5T2-C5′T3′** (**14a/b**), while **15a** is a minor product from the reaction and not separable by chromatographic methods from **C5T2-C5′T2′**, **16a**. (Figs. S49 and S50, Supplementary data). The formation of the 2,2′-bithienyl complexes **16a/b** in low yields is unexpected from the 2,3′-bithienyl substrate. The unprecedented formation of a 2,2′-bithienyl spacer indicates the cleaving of the inter-ring T2-T3′ bithienyl bond and the formation of a T2-T2′ bithienyl bond to give the known complexes [{M(CO)$_5$C(OEt)}$_2$-5,5′-(2,2′-BT)] (M = W, Cr) [6].

Scheme 4 highlights some intermediates that are believed to play an important role during bond-breaking and bond-making conversions. Firstly, the bond breaking and bond formation processes occur between organolithium reagents and metal acylates present in the reaction mixture. For the bond breaking we propose that all active α-positions must be occupied by metal acylate moieties (*vide infra*) as a prerequisite to activate a β-position. From previous work with thiophene by Aoki and co-workers and with our studies to prepare chelated biscarbene complexes, we found that a metalpentacarbonyl acylate fragment in the α-positions enhances the reactivity of adjacent β-positions, but at the same time protects the acyl carbon against nucleophilic attack [26]. As a result, we propose the presence of a trisacylate intermediate with two metal acylate fragments on the C2′ and C5′ positions of the T3′ ring. Furthermore, support for this intermediate is found in the isolation of **19a** which could only have resulted from the partial oxidation of an unstable triscarbene complex **18a** (Scheme 1). This requires the presence of the postulated trisacylate. The trisacylate renders the C3′ position (a β-position) of the T3′ ring the most reactive remaining site. Nucleophilic addition at this site, supported by steric congestion due to the presence of bulky metal carbonyl moieties, affords bond breaking. The fate of the butylthiophene fragment was not further investigated.

This leads to the formation of an 2,5-thienylene metal acylate dianion (blue, Scheme 4), a key intermediate for the bond-making step. Our explanation for the T2-T2′ bond making step is based on a reaction between the above dianion and a second C5T2-C5′T3′ bisacylate intermediate which represents the precursor of the major product **14a/b** of the reaction. In this case the T3′ ring contains a less active C3′ (β-position) compared with the T2 ring's more active C2 (α-position). The formation of a 2,2′-dithienylene inter-ring bond follows from a nucleophilic addition of the above generated dianion at the C2T2 site of the C5T2-C5′T3′ intermediate to give **16a/b**. The resulting β-lithiated dianion (red, Scheme 4) which forms as an intermediate has an active site available on the C5-position and will transmetallate [20] to generate more favoured 2,5-thienylenemonoacylate dianion and further facilitate the bond breaking nucleophilic addition.

FC complexes of Group 6 transition metals are readily oxidised by trace amounts of oxygen to give esters [6]. These reactions are further enhanced when the number of metal-carbene moieties on a common backbone increases [7,10]. The presence of an ester moiety therefore betrays the initial presence of a carbene centre where very reactive, and difficult to isolate, multicarbene complexes are present in reaction mixtures. An increase in ester moieties will lead to increased stability, and the oxidation usually ends with Fischer monocarbene complexes which are reasonably resistant to further oxidations during work up. Notable is the isolation and characterization of **19a** which provides proof of the *in situ* formation of a triscarbene complex **18a**, involving all three active α-positions of the 2,3′-bithienyl substrate (Scheme 1). Furthermore, the final monocarbene complex isolated gives insights into the relative reactivities of the different carbene sites. The most reactive site is on the inside position (C2′) of the thiophene ring bearing two carbene moieties (C2′/C5′) and will be oxidised first as is confirmed by the isolation of **17a**. It is also clear that the outside carbene unit on this thiophene ring is more reactive than the remaining carbene unit on the other thiophene ring as is confirmed by the molecular structure of **19a**.

Table 4
Chemical shifts (δ) of the biscarbene complexes and related complexes (^{1}H NMR/^{13}C NMR).

Complex	H/C2	H/C3	H/C4	H/C5	H/C2′	H/C3′	H/C4′	H/C5′	C_{carb}	C_{CO}[a]	OEt[b]/NR_2
10a (^{1}H)/(^{13}C)	7.87/130.4	/137.5	8.30/138.8	/158.9					/290.8	/202.3, 197.5	5.03, 1.69/78.7, 14.9
10b	7.77/129.4	/137.6	8.39/138.3	/155.8					/316.9	/223.1, 217.0	5.22, 1.70/76.2, 15.2
11a			7.48/	8.09/							4.99, 1.68/
11b			7.47/	8.18/							5.18, 1.70/
12a			7.10/	7.78/	7.56/		7.90/				4.72(C2),1.16(C2) 5.01(C5′),1.67(C5′)/
13ab	/155.4	/136.1	8.04/140.1	/155.4	7.19/123.1	/131.6	6.96/127.9	7.36/126.0	/304.6 (W), 317.7 (Cr)	203.0(W),196.6 (W),/223.4 (Cr),216.6 (Cr)	4.73 (C2),1.27 (C2)5.21 (C5), 1.70 (C5)/79.4 (W), 14.1 (W)76.4 (Cr), 15.1 (Cr)
13ba	n.o.	n.o.	7.97/140.0	n.o.	7.16/123.2	n.o.	7.00/127.5	7.38/126.5	/290.7 (W), 317.7 (Cr)	/202.4 (W), 197.3 (W), 223.8 (Cr), 215.3 (Cr),	4.73(C2), 1.39 (C2) 5.01(C5), 1.68 (C5)/78.8 (W), 14.9 (W) 76.4 (Cr), 14.6 (Cr)
14a	/147.3	7.38/125.6	8.15/143.3	/156.3	8.02/131.6	/136.1	8.26/137.0	/159.5	/291.1288.1	/202.5, 202.2, 197.6, 197.3	5.01(C5), 1.68 (C5) 5.03(C5′), 1.69(C5′)/78.9(C5), 78.4 (C5′)15.0(C5), 14.9(C5′)
14b	/136.0	7.40/125.6	8.24/142.6	/153.1	7.89/130.1	/146.3	8.36/137.1	/156.1	/317.2313.8	/223.3, 223.1 217.1, 216.8	5.19(C5), 1.70(C5) 5.22(C5′), 1.70(C5′)/76.6(C5), 76.0 (C5′)15.3(C5), 15.1(C5′)
15a	/128.3	7.04/126.8	7.04/126.4	7.34/127.5	/157.2	/136.4	7.98/139.5	/158.0	/305.8290.9	/203.4197.1, 196.4	4.99(C5′), 1.68(C5′) 4.79(C2′), 1.38(C2′)/79.4,(C5′),78.8 (C2′) 14.9,(C5′),14.2(C2′)
16a [24]	/145.4	8.09/142.6	7.48/127.0	/157.8	/145.4	8.09/142.6	7.48/127.0	/157.8	/288.5	/202.4, 197.4	5.00, 1.68/78.5, 15.0
16b [24]	/144.8	7.45/141.8	8.16/127.1	/154.3	/144.3	7.45/141.8	8.16/127.1	/154.3	/314.3	/223.4, 216.9	5.19, 1.70/76.0, 15.2
17a[*]			8.02/		7.61/		7.32/	7.37/			4.32(C2)[*],1.33(C2)[*] 5.02 (C5), 1.70 (C5)/
19a[*]	/145.3	7.61/130.7	8.11/141.7	/157.9	/133.4	/137.1	7.88/135.3	/138.2	/289.9	/202.6, 197.5 161.1*, 161.0*	4.99, 1.66 4.40[*], 4.36[*], 1.40[*], 1.36[*]/78.5, 15.0 76.7, 14.2 62.1, 14.1
20a	/137.6	6.50/117.4	7.07/123.3	/152.4	6.76/118.1	/134.3	7.29/119.9	/154.5	/250.0 249.8	/203.7, 203.6 198.2, 198.2	3.94, 3.30/53.9, 45.3

[a] Carbon chemical shifts for the carbonyls are reported with the first value being the chemical shift of the carbonyl trans to the carbene carbon, and the second the chemical shift of the carbonyls cis to the carbene carbon.

[b] Carbon chemical shifts for the ethoxy fragment are reported with the first value being value being the chemical shift of the methylene group, and the second the chemical shift of the methyl group.

[*] (O): C(O)Et.

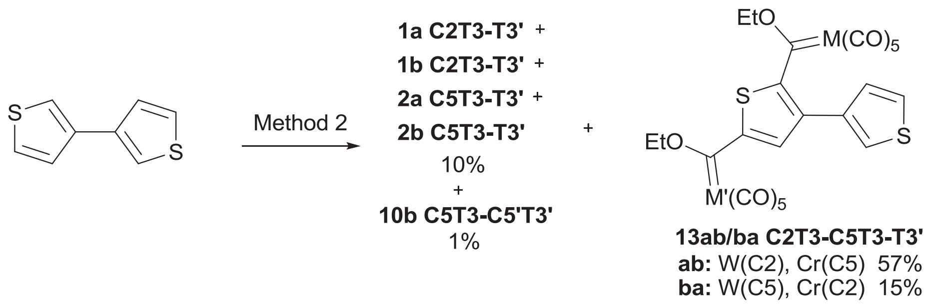

Scheme 3. Mixed metal biscarbene complexes from 3,3′-bithienyl substrates. **Method 2**: 1 eq *n*-BuLi, 1 eq M(CO)$_6$ in THF, 1 eq *n*-BuLi, 1 eq M′(CO)$_6$ in THF, 2 eq [Et$_3$O][BF$_4$] in DCM.

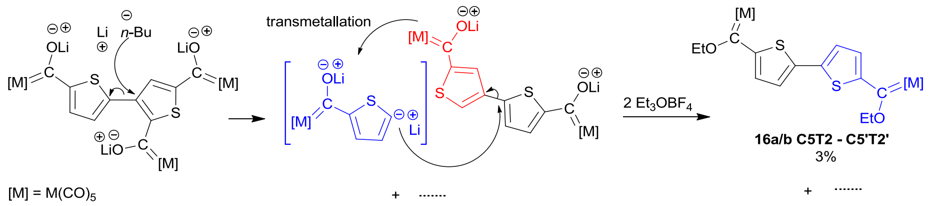

Scheme 4. The formation of 5,5′-biscarbene complexes with 2,2′-dithienylene spacers, **16a/b C5T2-C5′T2′**.

Aminolysis of the biscarbene complex **14a** (C5T2-C5'T3') was studied to compare electronic and steric properties of multiple methyl substituents of the nitrogen atoms with those of the amino monocarbene complexes **8a** and **9a**. Different electronic environments of amino substituents are emphasised by a further duplication of one of the chemical shifts of the methyl substituents in the biscarbene aminolysed product, **20a** (Figs.S58 and S59, Supplementary data).

The chemical shifts of the H4 protons, in 3,3′-bithienylene adjacent to the carbene substituents in the C5-positions, are most affected and practically the same for mono- (**2**) and biscarbene complexes (**10**). The corresponding mono- and biscarbene complexes of thiophene [7] show a large difference between these resonances (Δ*δ*± 0.18 ppm). When H4 resonances of the C2-monocarbene complexes (**1**) were compared with those of the C2,C2′-biscarbene complexes (**11**), the latter are found more downfield in each case. The H4 chemical shift of **13ab** and **13ba** (with both carbene substituents on the same thiophene ring of 3,3′-bithienyl) closely resemble the H4 shifts of the chromium thiophene (8.06 ppm) [7] and tungsten (7.97 ppm) biscarbene complexes [22], respec-

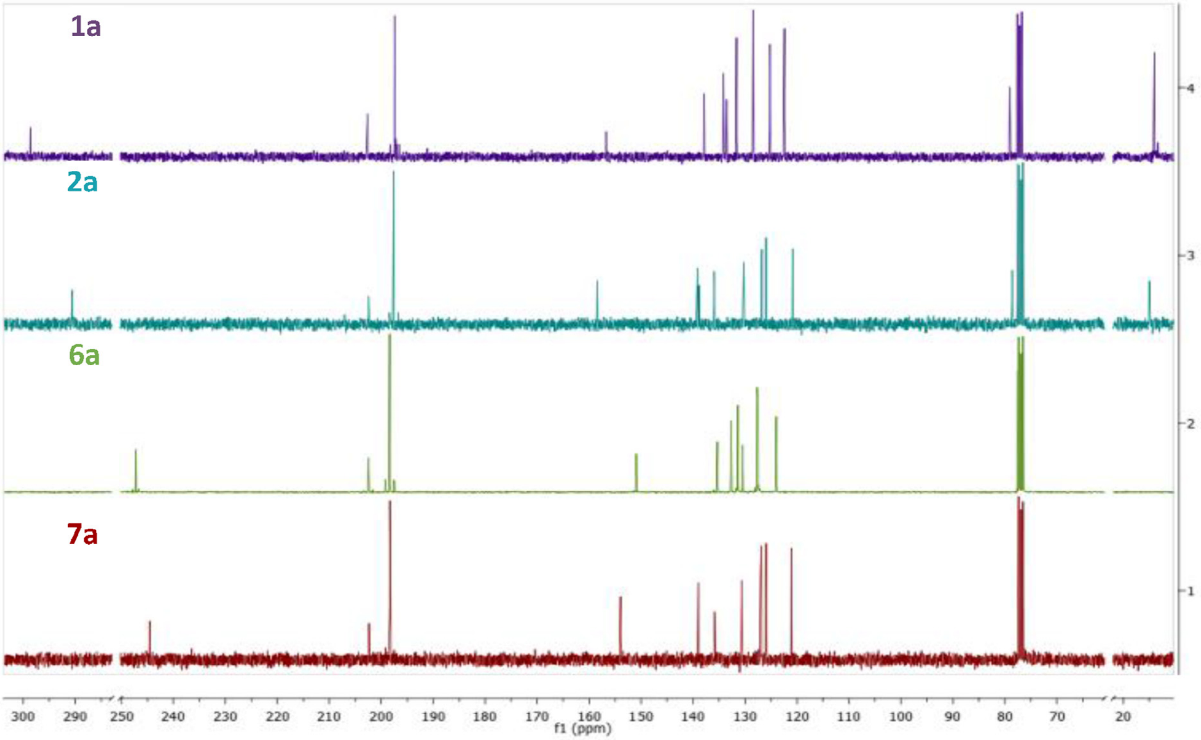

Fig. 5. ^{13}C NMR spectra of **1a**, **2a**, **6a** and **7a**.

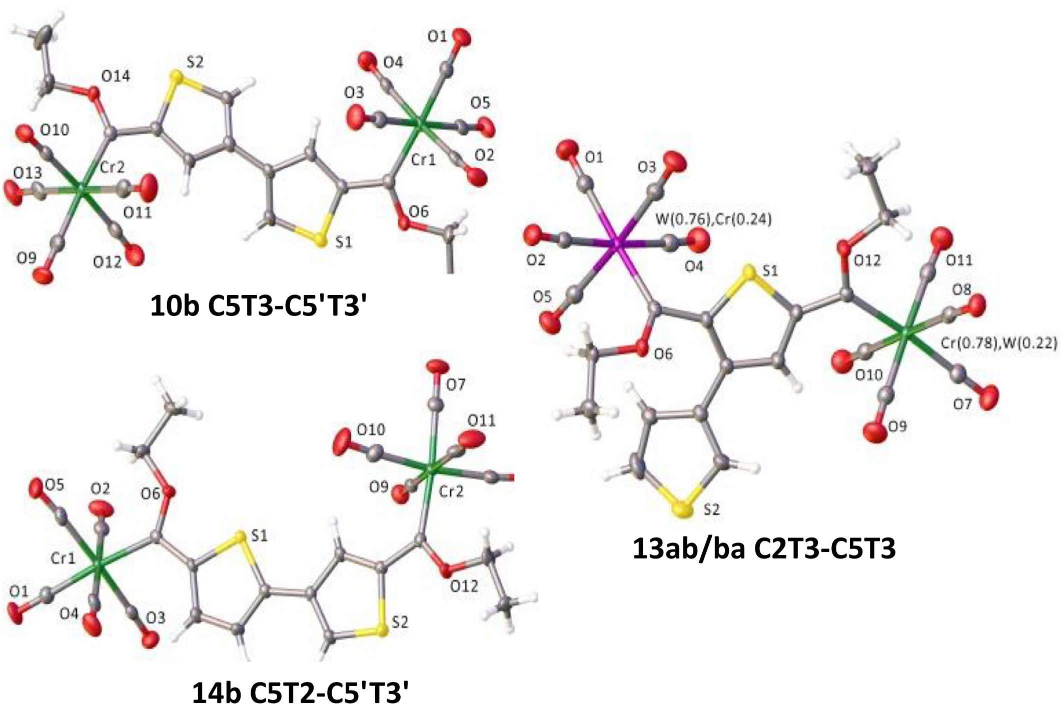

10b C5T3-C5'T3'

13ab/ba C2T3-C5T3

14b C5T2-C5'T3'

Fig. 6. The molecular structures with atom numbering of **10b**, **13ab/ba** and **14b** with atomic displacement ellipsoids shown at the 50% probability level.

Table 5
Selected bond lengths (Å), bond angles (°) and torsion angles (°) of the structures **10b**, **13ab/ba** and **14b**.

	10b(non-planar)	13ab/ba	14b
Bond lengths (Å)			
W/Cr–C_{carb}	2.047(3)	2.1247(19)[a]	2.075(3)
	2.051(3)	2.0835(18)[b]	2.054(3)
C_{carb}–C_{ipso}	1.461(3)	1.489(3)[a]	1.455(4)
	1.463(3)	1.469(3)[b]	1.464(4)
C_{carb}–O	1.323(3)	1.319(2)[a]	1.324(3)
	1.327(3)	1.325(2)[b]	1.331(3)
C2–C3	1.374(4)	1.389(3)	1.384(4)
C3–C4	1.420(3)	1.417(3)	1.401(4)
C4–C5	1.376(4)	1.375(3)	1.383(4)
C′2–C′3	1.367(4)	1.373(3)	1.373(4)
C′3–C′4	1.416(4)	1.457(3)	1.427(4)
C′4–C′5	1.372(4)	1.350(6)	1.382(4)
C—$C'_{interring}$	1.462(4)	1.471(3)	1.462(4)
Bond angles (°)			
C_{ipso}–C_{Carb}–O	104.8(2)	104.19(15)[a]	105.9(2)
	105.1(2)	104.95(15)[b]	104.6(2)
C_{ipso}–C_{Carb}–W/Cr	125.43(18)	121.40(13)[a]	124.84(19)
	125.22(18)	124.81(13)[b]	125.63(19)
W/Cr–C_{Carb}–O	129.79(18)	134.26(13)[a]	129.2(2)
	129.71(18)	130.23(13)[b]	129.73(19)
Torsion angles (°)			
W/Cr-C_{carb}-C_{ipso}-C_T	9.5(4)	-123.12(19)[a]	-1.2(4)
	7.1(4)	8.1(3)[b]	-13.4(5)
X_O-C_{carb}-C_{ipso}-C_T	-172.3(3)	52.9(3)[a]	178.9(3)
	-172.8(3)	-173.1(2)[b]	168.3(3)
C_X-O-C_{carb}-W/Cr	-4.6(4)	0.9(3)[a]	-3.0(4)
	-1.6(4)	-3.8(3)[b]	3.3(4)
C_{Tio}-C_{ipso}-C'_{ipso}-C'_T (inter-ring)	-145.0(3)	-156.8(3)	-3.4(4)
	-147.6(3)	-152.7(4)	176.0(3)

[a] C2-position : W(0.77), Cr(0.23).

[b] C5-position W(0.23), Cr(0.77) – first values in table apply to [a] and second to [b].

tively, as well as that of the thiophene mixed metal biscarbene complex (**21ab/ba**) (8.08 and 7.98 ppm). The methylene resonance of the ethoxy substituents of C5T3 mono- and C5T3-C5′T3′ biscarbene complexes are identical for the metal analogues with the trend Cr > W. The shifts of **13ab** and **13ba** at C5T3 are similar to those of the chromium and tungsten C5T3 mono- and C5T3-C5′T3′-bis-carbene complexes, respectively. The methylene proton chemical shifts of the C2T3 monocarbene complexes, as well as **13ab** and **13ba** at C2T3 are similar and independent of the nature of the metal carbonyl fragment. The chemical shifts of the carbene carbon in the ^{13}C NMR spectra are the furthest downfield and influenced by the nature of substituents and displays characteristic values for different transition metals. For example, the carbene carbon resonances of the C5T3 monocarbene complexes follow the trend from most to least deshielded **2b** > **2a** > **7b** > **7a**, while the ethoxycarbene C5 carbon resonate more downfield compared to the corresponding aminocarbene carbene carbon atom (Fig. 5). Considering the C2T3 monocarbene complexes, the same trend as for the analogous C5T3 monocarbene complexes is observed. The chemical shift of the chromium carbene carbon is the same irrespective of being in the C2- or C5-position in **13ab** and **13ba**, while in the case of tungsten they are site dependent and therefore differ.

Also significant is the electron withdrawing effect of the carbene fragment at the C2T3 and C5T3 positions on the *ipso*-carbon of thiophene which is the furthest downfield of the aromatic carbons. The chemical shift trend for *ipso*-carbons is **10** $\geq$ **2** > **1** > **7** > **6**, with resonances for tungsten complexes slightly more downfield compared to chromium.

Single crystal X-ray diffraction studies confirm the molecular structure of **10a** (*vide infra*), two structures for **10b** planar and non-planar (see Fig. S1 in Supplementary data), and the structures of **13ab/ba** and **14b** (Fig. 6). Selected bond distances, angles and torsion angles are listed in Table 5. Structural diffraction data for **10a** is included in the Supplementary data.

Complex **10b** crystallises as two sets of crystals which can be morphologically separated as purple needles and orange plates. The purple complex displays an almost *planar* bithienyl backbone with inter-ring torsion angles of −171.9(11)° and −171.6(11)°, compared to −145.0(3)° and −147.6(3)° for the more *distorted* orange complex. The difference in appearance of the crystals is a result of increased number of intermolecular hydrogen interactions in **10b** *planar* allowing closer columnar stacking with an intermolecular distance of 7.550 Å between bithienylene rings (Fig. S3, Supplementary data), compared to a distance of 13.439 Å in **10b** *non-planar*.

The molecular structure of **13ab/ba** is composed of 77% of the mixed metal biscarbene complexes where the tungsten fragment is bonded to C2T3 and the chromium fragment to C5T3. The other structural isomer which represents 22%, has the chromium fragment at C2T3 and tungsten fragment at C5T3. The remaining 1% of the crystal consists of the corresponding chromium biscarbene complex. Two averaged positions for the sulphur atom of the second thiophene ring is observed as a result of inter-ring rotation. The mixed metal biscarbene complex of thiophene, **21ab/ba** is composed of 39% W and 61% Cr at one metal site and 34% W and 66% Cr at the other metal site (see Fig. S1 in the Supplementary data).

The two thiophene rings are planar in the Cr biscarbene complex with a 2,2′-bithienylene spacer – the C2-C2′ bond lies across a centre of inversion [10]; a little less so in 2,3′-bithiophene (-3.4(4)° and 176.0(3)°, **14b**), but deviate considerably from planarity for 3,3′-bithienylene (−145.0(3) and −147.6(3) for **10b** ***non-planar.*** In the biscarbene complex of 2,3′-bithienylene, **14b**, the metal–carbene carbon bond distance for the carbene on the T2 ring is significantly longer (2.075(3) Å) than the corresponding distance on the T3′ ring (2.054(3) Å). The latter is the same as those observed in **10b** *non-planar*. A distance of 2.059(3) for this bond in the biscarbene complex of 2,2′-bithienylene falls within the range set by a T2 and a T3′ carbene in **14b**. The metal–carbene carbon bond distance of the ethoxy monocarbene complexes of 3,3′-bithienyl is longer compared to their 2,3′-bithienyl analogues, and both are longer compared to the 3,3′-bithienylene biscarbene complexes, respectively, for chromium and tungsten (with the bonds for the tungsten analogues being longer).

4. Conclusions

The presence of different α-activated sites in 3,3′- and 2,3′-bithienyl substrates was exploited to prepare a range of constitutional isomers of mono- and biscarbene bithienyl complexes of tungsten and chromium (**1**–**5**, **10**–**15**). The electronically favoured sites yielded preferentially ‘inside’ carbene complex formation (higher yields) in the case of the monocarbenes, while steric congestion in the biscarbene complexes resulted in higher yields/formation of only the outside-outside isomers. Notable is the formation of biscarbene complexes with the carbene ligands occupying the in- and outside position on the same thienyl ring of 2,3′-bithienyl, **15a T2-C2′T3′-C5′T3′**. In the case when ‘inside’ and ‘outside’ carbene formation on the same thiophene ring of the bithienyl substrate occurred, partial oxidation of the carbene moieties was observed to yield either a mono-ester, monocarbene complex **17a** (from corresponding biscarbene complex **13a**), or a diester, monocarbene complex **19a** to imply unstable triscarbene formation (**18a**). Unprecedented C—C bond cleavage and formation of the 2,3′-bithienyl substrate during the reaction yielded, unexpectedly, the known 2,2′-bithienyl carbene complexes **16**. The increased stabilising effect of aminocarbene substituents on the bithienyl substrates was investigated for the corresponding aminocarbene complexes **6**–**9**, **20**. Both NMR spectral and solid state structural data were used to evaluate the steric and electronic effects of the different carbene substitution sites on the bithienyl substrates. In general, the greater stability of the tungsten carbene complexes is reflected in the greater variety of complexes isolated and the higher yields obtained compared to the chromium analogues.

Acknowledgements

SL acknowledges the NRF for financial assistance (NRF grants 87788 and 95772). DIB gratefully acknowledges the National Research Foundation, South Africa (NRF 105740 and 105529), and Sasol Technology R&D Pty. Ltd., South Africa for financial support. The authors gratefully acknowledge Ms Madelien Wooding, University of Pretoria, for recording of the mass spectral data.

Appendix A. Supplementary data

Supplementary data to this article can be found online at https://doi.org/10.1016/j.poly.2018.10.060. CCDC 1847874–1847986 contains the supplementary crystallographic data, and can be obtained free of charge from the Cambridge Crystallographic Data Centre, 12 Union Road, Cambridge CB2 1EZ, UK; fax: (+44) 1223-336-033; or e-mail: deposit@ccdc.cam.ac.uk.

References

[1] (a) J. Roncali, Chem. Rev. 92 (1992) 711–738;
(b) D. Fichou (Ed.), Handbook of Oligo- and Polythiophenes, Wiley–VCH, Weinheim, Germany, 1999;
(c) P. Bäuerle, in: G. Wegner, K. Müllen (Eds.), Oligothiophenes in Electronic Materials: The Oligomeric Approach, Wiley-VCH, Weinheim, 1998;
(d) T.B. Rauchfuss, Prog. Inorg. Chem. 39 (1991) 256–329.
[2] L. Lancellotti, R. Tubino, S. Luzzati, E. Licandro, S. Maiorana, A. Papagni, Synth. Met. 93 (1998) 27–32.
[3] (a) M.M. Moeng, Terthienyl carbene complexes MSc. Dissertation, University of Pretoria, Pretoria, 2001;
(b) N.A. Van Jaarsveld, Synthesis and structure of modified thiophene biscarbene complexes, MSc. Dissertation, University of Pretoria, Pretoria, 2009.
[4] G.J. Visser, G.J. Heeres, J. Wolters, A. Vos, Acta Cryst. B 24 (1968) 467–473.
[5] R.M. Kellogg, A.P. Schaap, H.J. Wynberg, J. Org. Chem. 34 (1969) 343–346.
[6] S. Lotz, C. Crause, A.J. Olivier, D.C. Liles, H. Görls, M. Landman, D.I. Bezuidenhout, Dalton Trans. (2009) 697–710.
[7] Y.M. Terblans, M.H. Roos, S. Lotz, J. Organomet. Chem. 566 (1998) 133–142.
[8] A.I. Shatenshtein, A.G. Kamrad, I.O. Shapiro, Y.I. Ranneva, E.N. Zvyagintseva, Dokl. Akad. Nauk. SSSR 168 (1966) 364–366.
[9] S. Lotz, M. Landman, D.I. Bezuidenhout, A.J. Olivier, D.C. Liles, P.H. van Rooyen, J. Organomet. Chem. 690 (2005) 5929–5937.
[10] M. Landman, J. Ramontja, M. van Staden, D.I. Bezuidenhout, P.H. van Rooyen, D.C. Liles, S. Lotz, Inorg. Chim. Acta 363 (2010) 705–717.
[11] E.O. Fischer, A. Maasböl, Angew. Chem., Int. Ed. Engl. 3 (1964) 580–581.
[12] (a) N.A. Van Jaarsveld, D.C. Liles, S. Lotz, Dalton Trans. 39 (2010) 5777–5779;
(b) Z. Lamprecht, N.A. van Jaarsveld, D.I. Bezuidenhout, D.C. Liles, S. Lotz, Dalton Trans. 44 (2015) 19218–19231.
[13] V.G. Nenajdenko, D.V. Gribkov, V.V. Sumerin, E.S. Balenkova, Synthesis 1 (2003) 124–128.
[14] H. Meerwein, Org. Synth. 46 (1966) 113–115.
[15] Z. Lamprecht, S.G. Radhakrishnan, A. Hildebrandt, H. Lang, D.C. Liles, N. Weststrate, S. Lotz, D.I. Bezuidenhout, Dalton Trans. 46 (2017) 13983–13993.
[16] APEX3, (including SAINT and SADABS), BrukerAXS Inc., Madison, WI, 2016.
[17] G.M. Sheldrick, Acta Crystallogr., Sect. A: Found. Crystallogr. 71 (2015) 3–8.
[18] G.M. Sheldrick, Acta Crystallogr., Sect. C: Cryst. Struct. Commun. 71 (2015) 3–8.
[19] S. Lotz, N.A. van Jaarsveld, D.C. Liles, C. Crause, H. Görls, Y.M. Terblans, Organometallics 31 (2012) 5371–5383.
[20] B. Heckl, H. Werner, E.O. Fischer, Angew. Chem., Int. Ed. Engl. 7 (1968) 817–818.
[21] (a) D.M. Adams, Metal-Ligand and Related Vibrations, Edward Arnold Publishers Ltd, London, 1967, pp. 98–101;
(b) P.S. Braterman, Metal Carbonyl Spectra, Academic Press, London, 1975.
[22] M. Landman, R. Pretorius, B.E. Buitendach, P.H. van Rooyen, J. Conradie, Organometallics 32 (2013) 5491–5503.
[23] J.C.S. Costa, L.R. Gomes, L.M.N.B.F. Santos, J.N. Low, Acta Cryst. E66 (2010) o916.
[24] C. Crause, H. Görls, S. Lotz, Dalton Trans. (2005) 1649–1657.
[25] S. Maiorana, A. Papagni, E. Licandro, A. Persoons, K. Clay, S. Houbrechts, W. Porzio, Gazz. Chim. Ital. (1995) 377–379.
[26] S. Aoki, T. Fujimura, E.J. Nakamura, J. Am. Chem. Soc. 114 (1992) 2985–2990.
[27] For synthesis and characterisation of 21ab and 21ba, see Supplementary data, section SynS1, Scheme S1 and Figs. S60 and S61.